BIODEGRADABLE AND FUNCTIONALIZABLE 3D-PRINTED STIMULI-RESPONSIVE HYDROGELS

by
Altan Gümüşkaya
B.S., Chemistry, Boğaziçi University, 2022

Submitted to the Institute for Graduate Studies in
Science and Engineering in partial fulfillment of
the requirements for the degree of
Master of Science

Graduate Program in Chemistry
Boğaziçi University
2024

ACKNOWLEDGEMENTS

First and foremost, I would like to express my deepest gratitude to my thesis supervisor, Prof. Dr. Amitav Sanyal. His profound knowledge of chemistry and his patient guidance have been invaluable to me throughout my master's journey. I have had the privilege of learning from him not only during my thesis work but also during my undergraduate studies, where he taught several of my classes. His passion for teaching and research has inspired me greatly, and I am truly grateful for his mentorship and support over the years.

I would also like to extend my heartfelt thanks to Prof. Dr. Rana Sanyal and Assistant Prof. Özgül Gök Özatay for serving on my thesis jury. Prof. Dr. Rana Sanyal has been a constant presence throughout my academic journey, and her insightful feedback and encouragement have been instrumental in shaping my research. Their combined wisdom and support have been crucial in helping me navigate the challenges of my thesis.

A special thanks goes to İsmail Altınbaşak, who has been like a big brother to me. Currently, in the United States pursuing postdoctoral research, İsmail Abi has been a steadfast source of support, both academically and personally. His assistance at every step of this project, from the initial stages to the final touches, has been invaluable. He has guided me through the complexities of my research with the wisdom of a Jedi, and his encouragement has been the force that kept me going. His influence has extended beyond the lab, and I am profoundly grateful for his mentorship and friendship.

To Meltem Alkış, my lab sister, lab partner, and never-ending debater, I owe a debt of gratitude. Meltem has been my constant companion in the lab, always ready to lend a helping hand and engage in spirited discussions. Her support, whether in troubleshooting experiments or offering moral support, has been indispensable. Our collaborative efforts have made the lab a place of learning and growth, and I am thankful for her camaraderie and unwavering assistance.

Finally, I would like to acknowledge TÜBİTAK for providing the 2210-A scholarship during my master's period. This financial support has been critical in allowing me to focus on my research and pursue my academic goals. The opportunities and resources provided by TÜBİTAK have been instrumental in the completion of this thesis, and I am deeply appreciative of their support.

Thank you all for your guidance, support, and encouragement throughout this journey.

ABSTRACT

BIODEGRADBLE AND FUNCTIONALİZABLE 3D-PRINTED STIMULI-RESPONSIVE HYDROGELS

In this study, we developed innovative biodegradable and functionalizable 3D-printed stimuli-responsive hydrogels for advanced biomedical applications such as drug delivery and tissue engineering. Utilizing polyethylene glycol (PEG) polymers, the hydrogels incorporated redox-sensitive disulfide linkages for stimuli-responsive behavior. The custom-synthesized PEG-disulfide crosslinker (PEGSSDMa) provided stability and redox responsiveness. PEGMEMa enhanced porosity and swelling ratios, while PEGDMa added network stability.

The fabrication used extruder-based 3D printing for precision, with gellan gum increasing the viscosity of the hydrogel precursor solution to maintain structural fidelity. UV crosslinking post-printing enhanced mechanical integrity and resistance to dissolution. These hydrogels demonstrated a balanced combination of robustness and biodegradability, tailored to degrade at controlled rates.

The redox-responsive nature enabled targeted release of therapeutic agents in specific physiological environments, enhancing treatment efficacy and safety. Functionalizing hydrogels with bioactive molecules promoted cell adhesion, proliferation, and differentiation, essential for tissue regeneration. This study advances biomedical engineering by developing multifunctional hydrogels that integrate biodegradability, functionalizability, and stimuli-responsiveness, paving the way for new therapeutic strategies.

ÖZET

BİYOLOJİK OLARAK PARÇALANABİLEN VE FONKSİYONELLEŞTİRİLEBİLİR, 3D BASKILI, UYARANLARA DUYARLI HİDROJELLER

Bu çalışmada, ilaç taşıma ve doku mühendisliği gibi ileri biyomedikal uygulamalar için yenilikçi, biyobozunur ve fonksiyonelleştirilebilir 3D baskılı uyaranlara duyarlı hidrojeller geliştirdik. Polietilen glikol (PEG) polimerleri kullanılarak, hidrojeller uyaranlara duyarlı davranış için redoks-duyarlı disülfid bağları içerecek şekilde tasarlandı. Özel olarak sentezlenen PEG-disülfid çapraz bağlayıcı (PEGSSDMa) stabilite ve redoks duyarlılığı sağladı. PEGMEMa gözenekliliği ve şişme oranlarını artırırken, PEGDMa ağ stabilitesini sağladı.

Üretim sürecinde, hidrojel öncü çözeltisinin viskozitesini artırmak için gellan gum kullanılarak, yapı bütünlüğünü koruyan ekstrüder tabanlı 3D baskı teknolojisi kullanıldı. Baskı sonrası UV çapraz bağlama, mekanik bütünlüğü ve çözünmeye karşı direnci artırdı. Bu hidrojeller, belirli biyomedikal uygulamalara uygun şekilde kontrollü hızlarda bozunacak şekilde tasarlanmış, sağlamlık ve biyobozunurluğun dengeli bir kombinasyonunu sergiledi.

Redoks-duyarlı yapı, belirli fizyolojik ortamlarda terapötik ajanların hedeflenen salımını sağlayarak tedavi etkinliğini ve güvenliğini artırdı. Hidrojellerin biyoaktif moleküllerle fonksiyonelleştirilmesi, hücre adezyonu, proliferasyonu ve farklılaşmasını teşvik ederek doku rejenerasyonu için gerekli olan çok yönlü bir platform sundu. Bu çalışma, biyobozunurluk, fonksiyonelleştirilebilirlik ve uyaranlara duyarlılığı entegre eden çok işlevli hidrojeller geliştirerek biyomedikal mühendislikte önemli ilerlemeler sunmaktadır ve yeni terapötik stratejilerin önünü açmaktadır.

TABLE OF CONTENTS

ACKNOWLEDGEMENTS iii
ABSTRACT v
ÖZET vi
LIST OF FIGURES viii
LIST OF TABLES xi
LIST OF ACRONYMS/ABBREVIATIONS xii
1. INTRODUCTION 1
1.1. Smart Polymeric Materials for Biomedical Applications 1
1.2. 3D-Bioprinting of Polymeric Materials 4
1.3. 3D-Bioprinting Types and Parameters 8
1.4. Stimuli-Responsiveness and Functionability of Hydrogels 12
2. AIM OF THE STUDY 20
3. EXPERIMENTAL 23
3.1. Materials 23
3.2. Methods 23
3.3. Synthesis of Hydroxyethyl Methacrylate Disulfide (HEMA-SS) Acid 23
3.4. Synthesis of HEMA-SS-Terminated PEG Polymer 24
3.5. Preparation and Characterization of the HGs 24
3.6. Degradation of the HGs 25
4. RESULTS AND DISCUSSION 26
4.1. Synthesis and Characterization of Disulfide Methacrylate-Terminated PEG Polymer 26
4.2. Preparation and Characterization of HGs 29
4.3. Rheological Characterization of HGs 32
4.4. Degradation of HGs 34
4.5. Printability of HGs 36
5. CONCLUSION 39
REFERENCES 43
APPENDIX A: COPYRIGHT NOTICES 49

LIST OF FIGURES

Figure 1.1. Application of hydrogels in biomedical science [10]. 2

Figure 1.2. 3D models in CAD file and manufactured final model of the different cases [13]. 4

Figure 1.3. Scheme showing the bioprinting process [14]. 5

Figure 1.4. Schematic representation of different types of 3D bioprinting technology (A) Extrusion-based bioprinting, (B) Droplet-based bioprinting, (C) Fused deposition modeling, (D) Inkjet-based bioprinting, (E) Laser-assisted bioprinting, (F) Fused deposition modeling, (G) Stereolithography. [15]. 7

Figure 1.5. Scheme showing the possible strategies and applications of 3D-printed tumor microenvironment [22]. 12

Figure 1.6. An overview of biochemical, physical, and chemical stimuli used for stimuli-responsive polymers [24]. 13

Figure 1.7. Schematic illustration of dissolvable HGs [26]. 15

Figure 1.8. Schematic illustration of reduction-responsive intracellular drug delivery by the micelle structure [27]. 16

Figure 1.9. Schematic diagram of the co-axial 3D printing of core-shell fibers/scaffolds for localized cancer therapy. Drug released from the core hydrogels after NIR-induced reversible sol-gel transition [34]. 19

Figure 4.1. Synthesis of disulfide-containing PEGDMa crosslinker..... 27

Figure 4.2. (a) ^{1}H NMR and (b) ^{13}C NMR spectra of the HEMA-disulfide acid..... 27

Figure 4.3. (a) 1H NMR and (b) 13C NMR spectra of the HEMA-SS-terminated PEG polymer..... 28

Figure 4.4. FTIR spectrum of (a) 4K PEG and (b) PEGSSDMa..... 29

Figure 4.5. Photographic image of a wet HG1 hydrogel sample in front (a) and side (b)..... 31

Figure 4.6. SEM pictures of hydrogels with different ratios (a) HG1, (b) HG2, and (c) HG3..... 31

Figure 4.7. Swelling of HG1, HG2, and HG3 hydrogels. 31

Figure 4.8. (a) Strain sweep and (b) frequency sweep test of HG1 hydrogel solution. 32

Figure 4.9. (a) Strain sweep and (b) frequency sweep test of HG1 before and after crosslinking. 33

Figure 4.10. Photographic image of HG1 hydrogel sample in water (a) and in 10 mM DTT solution (b). 35

Figure 4.11. Photographic image of HG2 hydrogel sample in water (a) and in 10 mM DTT solution (b). 35

Figure 4.12. Time sweep test of HG1 hydrogel in the presence and absence of DTT.... 36

Figure 4.13. Strain sweep test of hydrogel solutions with different GG ratios (BInk1 and BInk2). 37

Figure 4.14. Photographic image of grit pattern up front (a), thick grit pattern on the side (b) made by HG1 and canal way (c) made outer filling with BInk1 and inner filling with HG1. 38

Figure A.1. Permission for Figure 1.1 from Ref [10]. 49

Figure A.2. Permission for Figure 1.2 from Ref [13]. 49

Figure A.3. Permission for Figure 1.3 from Ref [14]. 50

Figure A.4. Permission for Figure 1.4 from Ref [15]. 50

Figure A.5. Permission for Figure 1.5 from Ref [22]. 51

Figure A.6. Permission for Figure 1.6 from Ref [24]. 51

Figure A.7. Permission for Figure 1.7 from Ref [26]. 52

Figure A.8. Permission for Figure 1.8 from Ref [27]. 52

Figure A.9. Permission for Figure 1.9 from Ref [36]. 53

LIST OF TABLES

Table 4.1. Hydrogels with different PEGSSDMa and PEGDMa ratios..... 30

Table 4.2. Hydrogels with different gellan gum (GG) ratios 37

LIST OF ACRONYMS/ABBREVIATIONS

3D	Three dimensional
DCM	Dichloromethane
DTT	1,4-Dithiothreitol
FTIR	Fourier transform infrared (FTIR)
GG	Gellan gum
HG	Hydrogel
HEMA	Hydroxyethyl methacrylate
HEMA-SS	Hydroxyethyl methacrylate disulfide acid
LAP	Lithium phenyl-2,4,6-trimethylbenzoylphosphinate
NG	Nanogel
NMR	Nuclear magnetic resonance
PEG	Poly(ethylene glycol)
PEGMEMA	Poly(ethylene glycol) methyl ether methacrylate
PEGSSDMA	Poly(ethylene glycol) disulfide dimethacrylate
PEGDMA	Poly(ethylene glycol) dimethacrylate
PEO	Poly(ethylene oxide)
RAFT	Reversible addition-fragmentation chain transfer
SEC	Size-exclusion chromatography
SEM	Scanning electron microscopy
THF	Tetrahydrofuran

1. INTRODUCTION

1.1. Smart Polymeric Materials for Biomedical Applications

Biomedical research has made extensive use of polymeric materials because of their remarkable physical and chemical characteristics as well as their functional qualities for a variety of uses [1-4]. Aside from the specific qualities needed for the intended use, polymeric materials used in biomedical applications should satisfy several general standards, such as biodegradability and biocompatibility. Smart polymers are designed to undergo reversible or irreversible changes in their physical or chemical properties in response to environmental triggers like temperature [1], pH [2], light [3], and magnetic fields [4]. The underlying molecular architecture of smart polymers is meticulously designed to facilitate these transitions, allowing for precise control over their behavior and functionality. This responsiveness is not merely a passive characteristic but a highly engineered feature that has opened new avenues in applications ranging from drug delivery systems [5] to environmental sensing [6] and biomedical engineering [7]. The potential of these materials to self-heal, shape-shift, and modulate their properties on demand represents a significant leap forward, pushing the boundaries of what can be achieved in fields that require high precision and adaptability. The integration of smart polymers into complex systems offers unprecedented levels of customization, making them suitable for a wide range of tailored applications.

Among the various forms of smart polymeric materials, hydrogels stand out due to their exceptional ability to mimic natural tissue environments [8], thanks to their high-water content and versatile structural properties. Hydrogels are three-dimensional, cross-linked polymeric networks capable of absorbing and retaining significant amounts of water while maintaining their structural integrity. This unique combination of properties makes hydrogels particularly attractive for biomedical applications, including tissue engineering, wound healing [9], and drug delivery that can be seen in Figure 1.1. The stimuli-responsive nature of smart hydrogels enables them to undergo substantial changes in their physical state or chemical composition in response to specific external stimuli. Hydrogels which are thermo-responsive can change their solubility or swelling behavior in response to changes

in temperature, whereas hydrogels that are pH-responsive can modify their network structure and ionization state in response to changes in ambient pH. This inherent adaptability allows hydrogels to be finely tuned for specific applications, providing precise control over their behavior and interactions within biological environments.

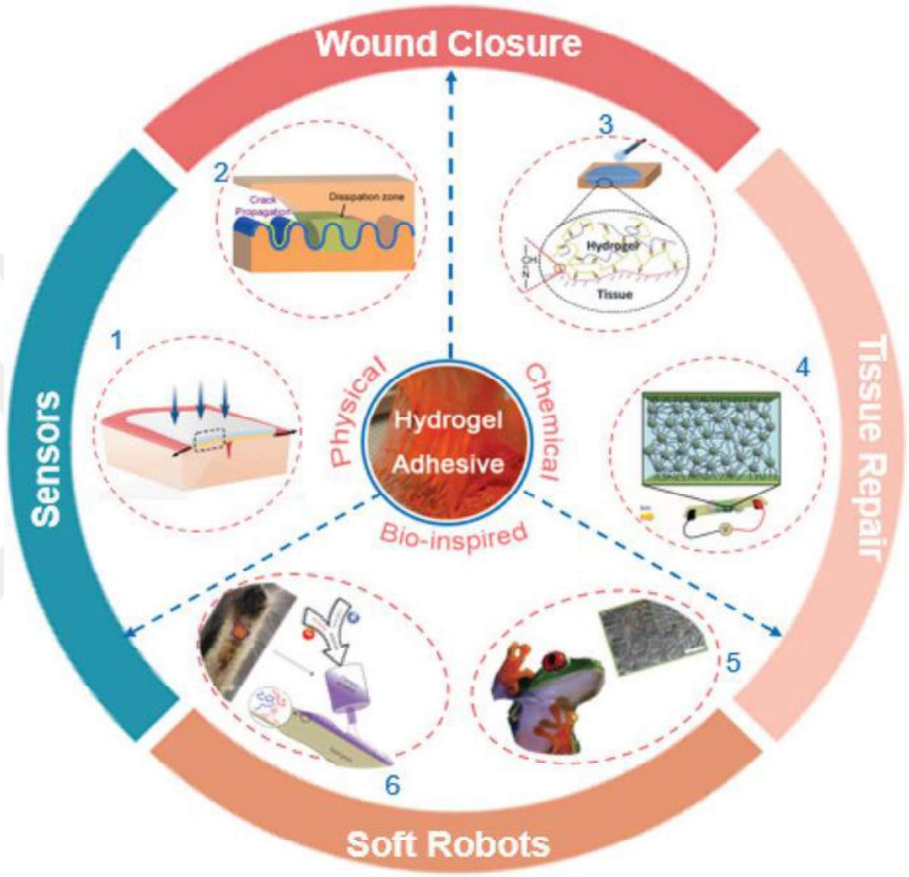

Figure 1.1. Application of hydrogels in biomedical science [10].

The benefits of using hydrogels extend far beyond their responsive capabilities, encompassing aspects of biocompatibility, biodegradability, and mechanical properties that are essential for their successful application in biomedical fields. Hydrogels can be engineered to degrade within the body over a predetermined period, which is particularly advantageous for temporary medical implants or scaffolds used in tissue regeneration. Their high-water content not only imparts softness and pliability, mimicking the extracellular matrix of natural tissues, but also facilitates nutrient diffusion and waste removal, which are crucial for cell survival and function. Furthermore, hydrogels can be functionalized with various chemical groups to enhance their interaction with biological tissues or to incorporate

bioactive molecules that promote healing or prevent infection [11]. One proactive method of managing wounds is to load hydrogels used in wound dressings with antimicrobial drugs that release in reaction to stimuli associated to infection. Similarly, in drug delivery applications, hydrogels can encapsulate therapeutic agents within their network and release them in a controlled manner, reducing the frequency of administration and improving patient compliance. The versatility and tunability of hydrogels underscore their potential to address complex medical challenges, making them indispensable tools in the advancement of regenerative medicine and therapeutic delivery systems.

The integration of smart polymeric materials into 3D printing and bioprinting technologies has opened new frontiers in biomedical engineering and material science [12]. These advanced materials, with their unique ability to respond to external stimuli, offer unprecedented levels of control and functionality, enabling the creation of complex, patient-specific structures [13] that can adapt to changing environmental conditions. Figure 1.2 shows different 3D models and manufactured constructs according to different cases. Hydrogels, in particular, have emerged as versatile and highly adaptable materials, providing numerous benefits in applications ranging from tissue engineering to drug delivery. The combination of smart hydrogels with 3D printing and bioprinting technologies has revolutionized the field, offering exciting new possibilities for the development of personalized medical solutions and advanced therapeutic devices. As research in this area continues to advance, it is expected that the use of smart polymeric materials in combination with cutting-edge fabrication technologies will lead to the development of innovative and highly effective treatments for a wide range of medical conditions, ultimately improving patient outcomes and quality of life.

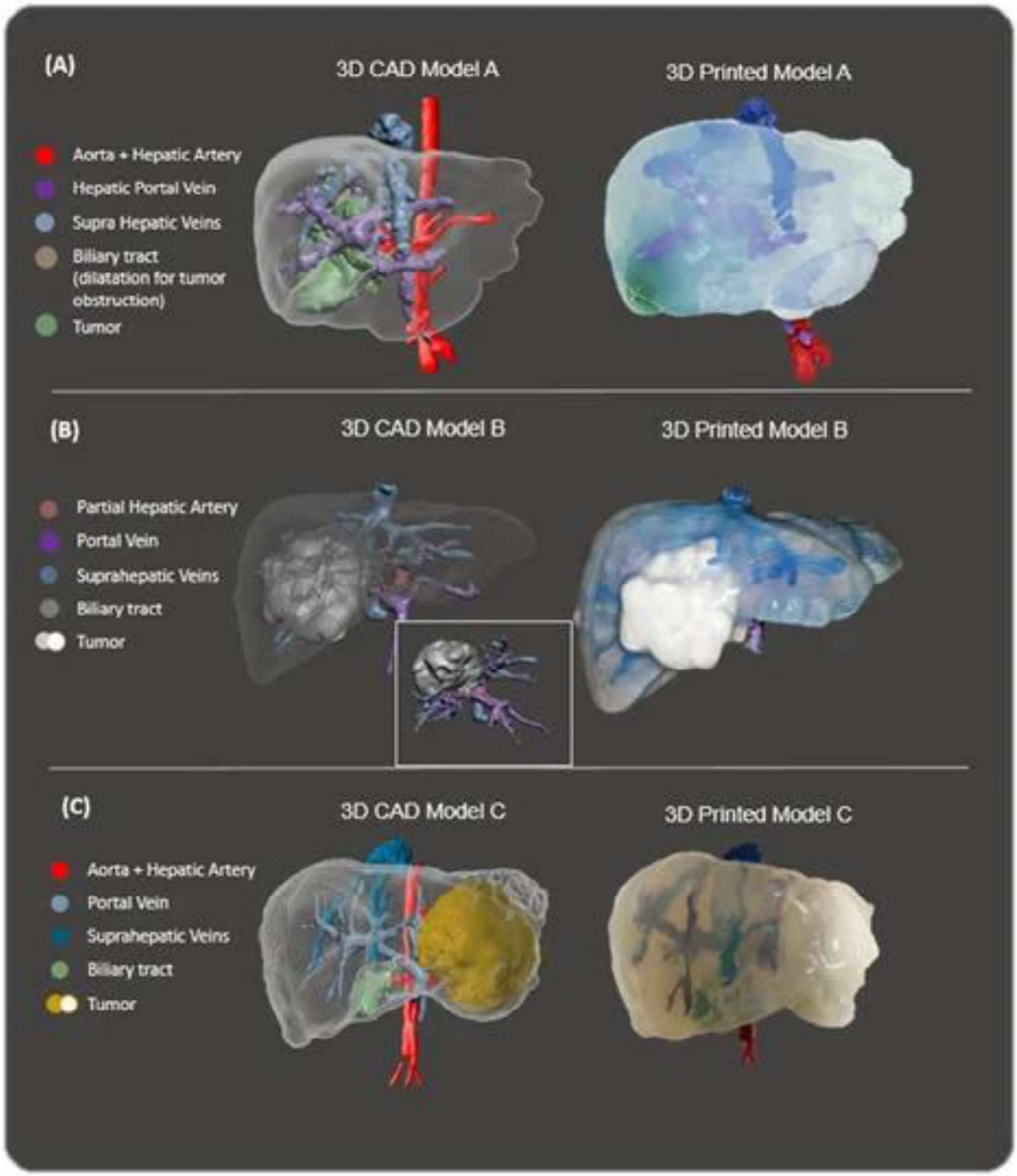

Figure 1.2. 3D models in CAD file and manufactured final model of the different cases [13].

1.2. 3D-Bioprinting of Polymeric Materials

The advent of 3D printing technology has dramatically transformed manufacturing and engineering fields, offering unprecedented levels of customization and precision. Initially developed in the late 20th century, traditional 3D printing, or additive manufacturing,

involved the layer-by-layer deposition of materials to create three-dimensional objects based on digital designs. This approach provided significant advantages over conventional manufacturing methods, including reduced waste, the ability to create complex geometries, and rapid prototyping capabilities. Early applications of 3D printing focused primarily on the fabrication of plastic and metal components for industrial and consumer products. However, as the technology evolved, researchers began to explore its potential in the biomedical field, leading to the emergence of bioprinting a specialized branch of 3D printing dedicated to creating biological tissues and structures using bioinks composed of living cells and biocompatible materials [14]. Figure 1.3 shows bioink which includes cell-laden GG/PEGDA DN hydrogels.

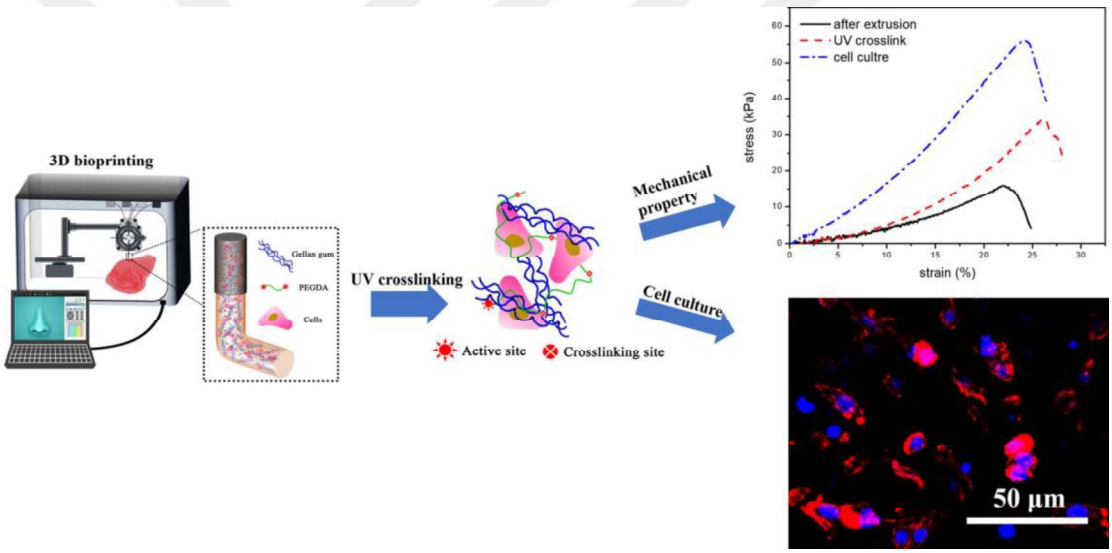

Figure 1.3. Scheme showing the bioprinting process [14].

The transition from traditional 3D printing to bioprinting involved several key advancements in both materials' science and printing technologies. One of the primary challenges in bioprinting is the development of suitable bioinks that can support cell viability, proliferation, and differentiation while maintaining the structural integrity of the printed constructs. Polymeric materials, particularly hydrogels, have played a crucial role in addressing these challenges due to their tunable properties and biocompatibility. Hydrogels, as discussed in the previous chapter, are highly hydrated polymeric networks that can mimic the extracellular matrix of natural tissues, providing a supportive environment for cell growth. The ability to modify hydrogels with functional groups and responsive elements

further enhances their suitability for bioprinting applications, enabling the creation of dynamic and multifunctional tissue constructs.

In addition to advancements in materials, the evolution of 3D printing technologies has been pivotal in the development of bioprinting. Early 3D printers utilized methods such as stereolithography (SLA) (Figure 1.4g) and fused deposition modeling (FDM) (Figure 1.4c and f) to create objects from thermoplastic materials [15]. While these techniques were effective for fabricating rigid structures, they were not suitable for printing soft, hydrated materials like hydrogels. To overcome this limitation, researchers developed new printing techniques specifically designed for bioprinting, such as inkjet bioprinting (Figure 1.4d), extrusion-based bioprinting (Figure 1.4a), and laser-assisted bioprinting (Figure 1.4e). These technologies enable the precise deposition of bioinks in predefined patterns, allowing for the creation of complex, multicellular structures with high spatial resolution.

The use of 3D bioprinting for tissue engineering and regenerative medicine has shown great promise in addressing some of the most pressing medical challenges. One of the key advantages of bioprinting is its ability to create patient-specific tissue constructs based on medical imaging data, such as CT scans or MRI images [13]. This level of customization is particularly important for applications such as bone and cartilage repair, where the geometry and mechanical properties of the printed constructs must match the patient's anatomy. By using bioprinting to create personalized implants and scaffolds, it is possible to improve the integration and functionality of these devices, leading to better clinical outcomes.

In addition to tissue engineering, bioprinting has also been explored for the creation of organ-on-a-chip devices [16], which are small, microfluidic systems that mimic the physiological functions of human organs. These devices offer a powerful platform for studying disease mechanisms, drug interactions, and toxicity in a controlled and reproducible manner. The use of smart hydrogels in bioprinting organ-on-a-chip devices allows for the creation of dynamic microenvironments that can better replicate the complex interactions between different cell types and tissues. For example, bioprinted liver-on-a-chip devices can be used to study liver metabolism and drug toxicity, providing valuable insights into the safety and efficacy of new therapeutics.

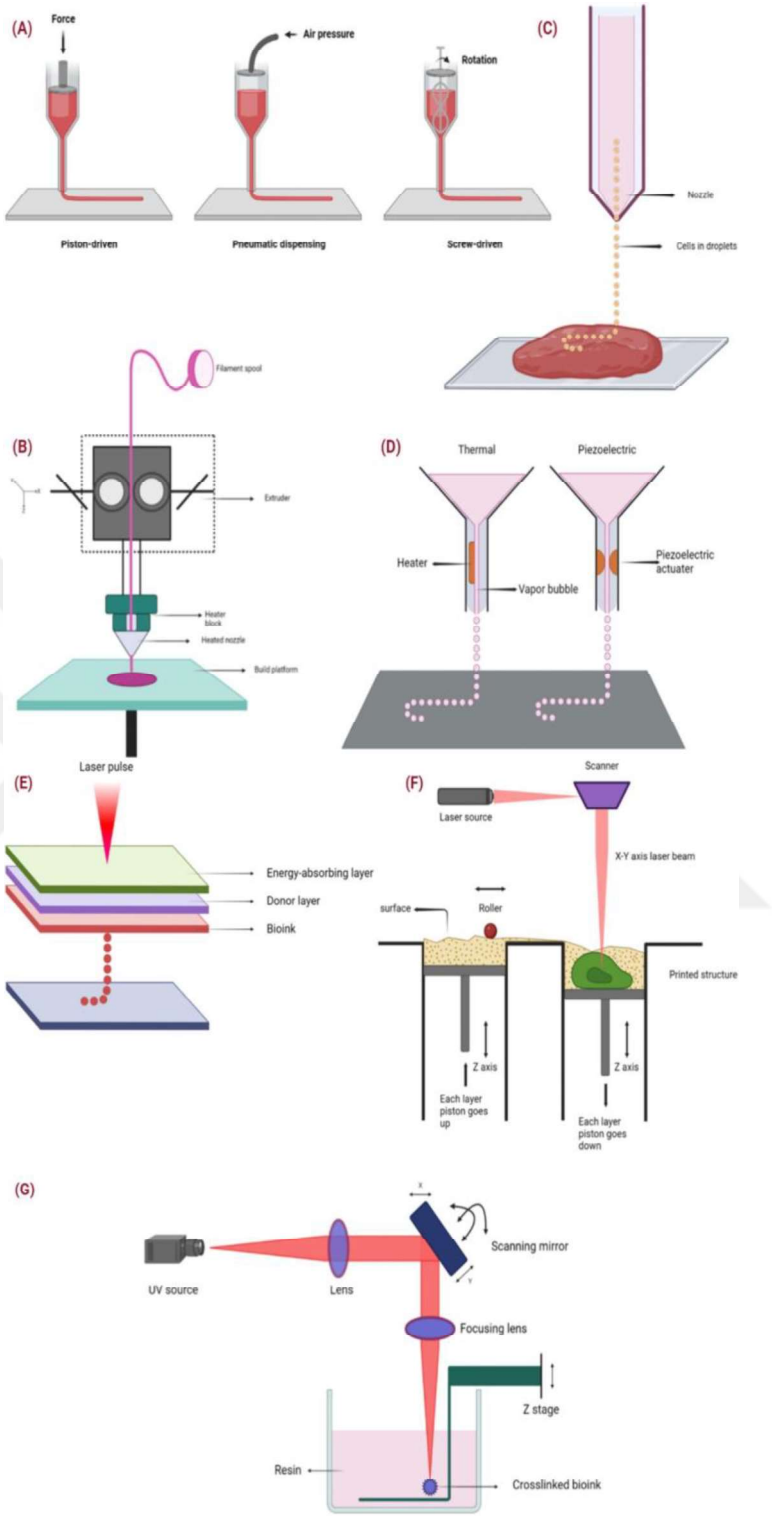

Figure 1.4. Schematic representation of different types of 3D bioprinting technology (A) Extrusion-based bioprinting, (B) Droplet-based bioprinting, (C) Fused deposition modeling, (D) Inkjet-based bioprinting, (E) Laser-assisted bioprinting, (F) Fused deposition modeling, (G) Stereolithography [15].

The combination of bioprinting technology with advanced imaging and computational modeling techniques has further enhanced the potential of 3D bioprinting for biomedical applications. By integrating data from imaging modalities such as MRI and CT with computational models, it is possible to create highly accurate and patient-specific designs for bioprinted constructs. This approach allows for the optimization of the mechanical and biological properties of the printed tissues, ensuring that they meet the specific requirements of each patient. Moreover, the use of computational models to simulate the behavior of bioprinted constructs under physiological conditions can provide valuable insights into their performance and help guide the design process.

1.3. 3D-Bioprinting Types and Parameters

The field of 3D bioprinting has rapidly evolved, leveraging advancements in printing technologies and materials science to create complex, functional biological structures. This chapter delves into the various types of 3D bioprinting technologies and the critical parameters that influence the success and functionality of bioprinted constructs. Building on the previous discussions on smart polymeric materials and their integration into bioprinting, this chapter explores the technical aspects and specific examples of different bioprinting methodologies.

Inkjet bioprinting is one of the earliest and most widely used bioprinting techniques. It operates on a drop-on-demand principle, where droplets of bioink are precisely ejected onto a substrate to form a 3D structure. The technology is adapted from traditional inkjet printing, but with modifications to handle biological materials. Inkjet bioprinters can be either thermal or piezoelectric. Thermal inkjet bioprinting uses localized heating to create vapor bubbles that force droplets out of the nozzle. Although this method provides high-resolution printing and can handle low-viscosity bioinks, the heat generated may affect cell viability. In contrast, piezoelectric inkjet bioprinting applies an electric charge to a piezoelectric crystal, causing it to deform and eject a droplet of bioink. This method operates at lower temperatures, which is more conducive to maintaining cell viability. Inkjet bioprinting is particularly suited for applications requiring high precision and small-scale constructs, such as microtissues and

organ-on-a-chip devices. However, the technique is limited by the viscosity of the bioinks that can be used, typically favoring low-viscosity formulations.

Extrusion-based bioprinting is a versatile and widely adopted method that involves the continuous deposition of bioink through a nozzle to create 3D structures. This technique can handle a wide range of bioink viscosities, making it suitable for printing both soft hydrogels and more viscous materials. Pneumatic extrusion utilizes air pressure to push bioink through the nozzle, providing good control over the flow rate and is suitable for a variety of bioinks, including those with high viscosities. Mechanical extrusion employs a mechanical screw or piston to extrude the bioink, achieving higher precision and consistency in bioink deposition, making it ideal for creating more complex structures. Extrusion-based bioprinting is advantageous for fabricating large, cell-laden constructs such as tissue scaffolds [14] and organ models [17]. Its ability to print high-viscosity bioinks allows for the creation of robust and stable structures, which are essential for certain biomedical applications.

Laser-assisted bioprinting is a high-resolution technique that uses laser pulses to transfer bioink from a donor substrate to a collector substrate. This method is contactless, reducing the risk of contamination and mechanical stress on the cells. In Laser-Induced Forward Transfer (LIFT), a pulsed laser beam is focused on a donor substrate coated with bioink. The laser energy creates a high-pressure bubble that propels a droplet of bioink onto the collector substrate. This method allows for precise placement of cells and materials, making it ideal for creating intricate tissue structures and microarrays. LAB is particularly useful for applications requiring high spatial resolution and precision, such as neural tissue engineering and the creation of microvascular networks [18]. However, the technique is limited by the need for specialized equipment and the relatively slow printing speeds compared to other bioprinting methods.

Stereolithography bioprinting uses light to polymerize a photosensitive bioink, layer by layer, to build a 3D structure. This technique offers high resolution and the ability to create complex geometries with smooth surfaces. Digital Light Processing (DLP), a variation of SLA, uses a digital light projector to polymerize entire layers of bioink at once, significantly speeding up the printing process while maintaining high resolution. SLA bioprinting is particularly suited for creating detailed scaffolds and complex tissue constructs. Its ability

to produce high-resolution features makes it a valuable tool for applications in tissue engineering and regenerative medicine [19].

The success and functionality of bioprinted constructs are influenced by various parameters, including bioink properties, printing conditions, and post-printing processes. Understanding and optimizing these parameters is crucial for achieving desired outcomes. The viscosity of the bioink affects its printability and the resolution of the printed structures. Low-viscosity bioinks are suitable for inkjet and laser-assisted bioprinting, while higher viscosities are better handled by extrusion-based methods. The ideal viscosity depends on the printing technique and the desired application. The rate at which the bioink transitions from a liquid to a gel state is critical for maintaining the shape and structural integrity of the printed construct. Rapid gelation is necessary to prevent the collapse of structures, especially in gravity-influenced environments. The bioink must support cell viability and function during and after the printing process. Factors such as shear stress, temperature, and exposure to light or chemicals must be carefully controlled to avoid damaging the cells.

The resolution of the bioprinter, determined by the nozzle diameter or laser spot size, affects the precision and detail of the printed structures. Higher resolution enables the creation of fine features and intricate designs, which are essential for certain applications. The printing speed influences the overall fabrication time and the quality of the printed construct. Faster printing speeds can lead to reduced resolution and accuracy, while slower speeds may result in better detail but longer production times. Maintaining appropriate environmental conditions, such as temperature and humidity, is crucial for preserving bioink properties and cell viability during the printing process. Specialized bioprinters may include features like temperature-controlled print beds and enclosed printing chambers to optimize these conditions.

After printing, additional crosslinking processes may be required to enhance the mechanical strength and stability of the construct. Crosslinking can be achieved through chemical, thermal, or photoinitiated methods, depending on the bioink composition. Bioprinted constructs often require a period of maturation in culture to promote cell growth, differentiation, and tissue formation. This process involves providing appropriate

biochemical and mechanical cues to guide tissue development and achieve the desired functionality.

Bioprinting has been extensively explored for creating tissue scaffolds that support cell growth and tissue regeneration. For instance, bioprinted scaffolds composed of hydrogels and biodegradable polymers can be used to repair bone and cartilage defects [20]. These scaffolds provide a temporary structure that cells can attach to and proliferate within, eventually being replaced by natural tissue. Organ-on-a-chip devices are microfluidic systems that replicate the physiological functions of human organs. Bioprinting enables the precise placement of cells and materials within these devices, creating complex tissue architectures that mimic the interactions between different cell types and tissues. These devices are valuable for drug testing, disease modeling, and studying organ-level functions in a controlled environment.

Bioprinting allows for the creation of patient-specific implants and prosthetics based on medical imaging data. For example, bioprinted bone implants can be designed to match the exact shape and mechanical properties of the patient's bone, improving integration and functionality [21]. Similarly, bioprinted prosthetic limbs can be tailored to the patient's anatomy, providing a better fit and enhanced performance. Bioprinted tumor models provide a more accurate representation of the tumor microenvironment compared to traditional 2D cell cultures. These models can be used to study cancer progression, metastasis, and the response to various treatments [22]. Bioprinting enables the creation of heterogeneous tumor structures that include different cell types and extracellular matrix components, offering a more realistic platform for drug testing and personalized medicine.

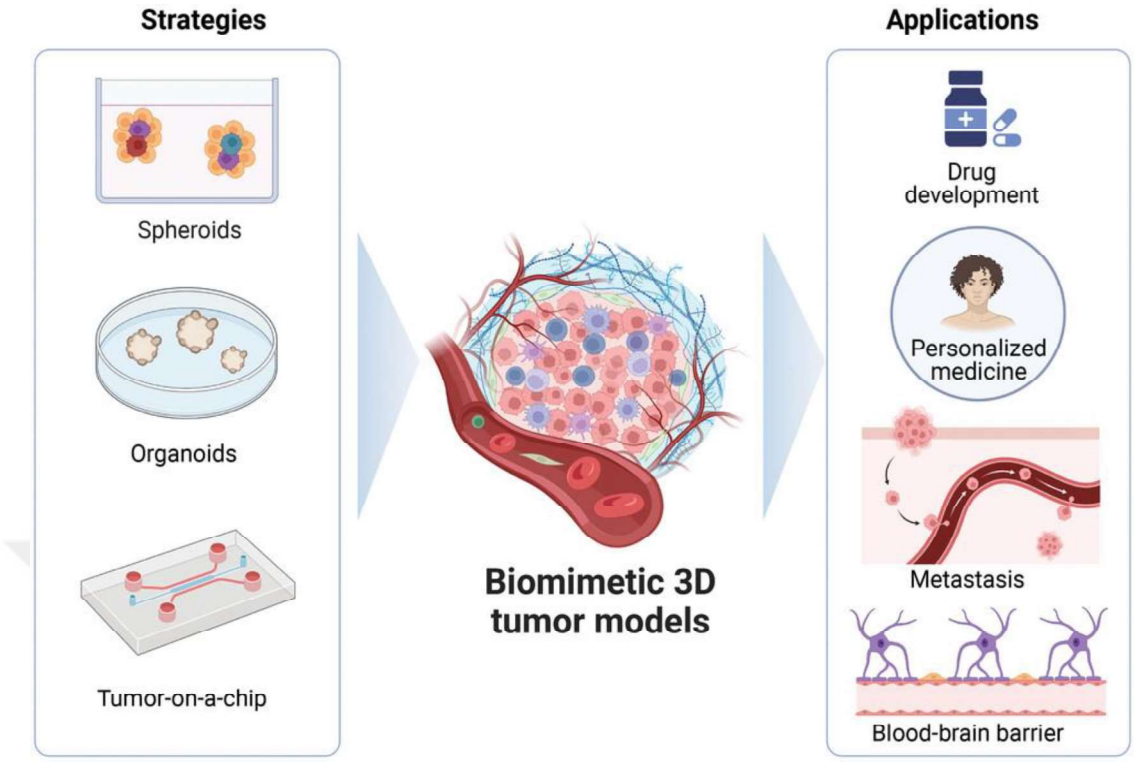

Figure 1.4. Scheme showing the possible strategies and applications of 3D-printed tumor microenvironment [22].

One of the major challenges in tissue engineering is the creation of vascularized tissues that can support the transport of nutrients and oxygen to cells [23]. Bioprinting techniques, such as coaxial extrusion and laser-assisted bioprinting, have been developed to create vascular networks within tissue constructs. These vascularized tissues are crucial for the development of larger and more complex organs, such as the liver and kidneys.

1.4. Stimuli-Responsiveness and Functionability of Hydrogels

In the expansive realm of biomaterials, hydrogels have garnered significant attention due to their versatile properties and potential applications in various biomedical fields. This chapter focuses on the stimuli-responsiveness and functionality of hydrogels, with a particular emphasis on the underlying chemistry that imparts these materials with their unique properties. Building on the foundational knowledge presented in previous chapters, this section delves deeper into the chemical mechanisms that enable hydrogels to respond to environmental stimuli and perform specific functions.

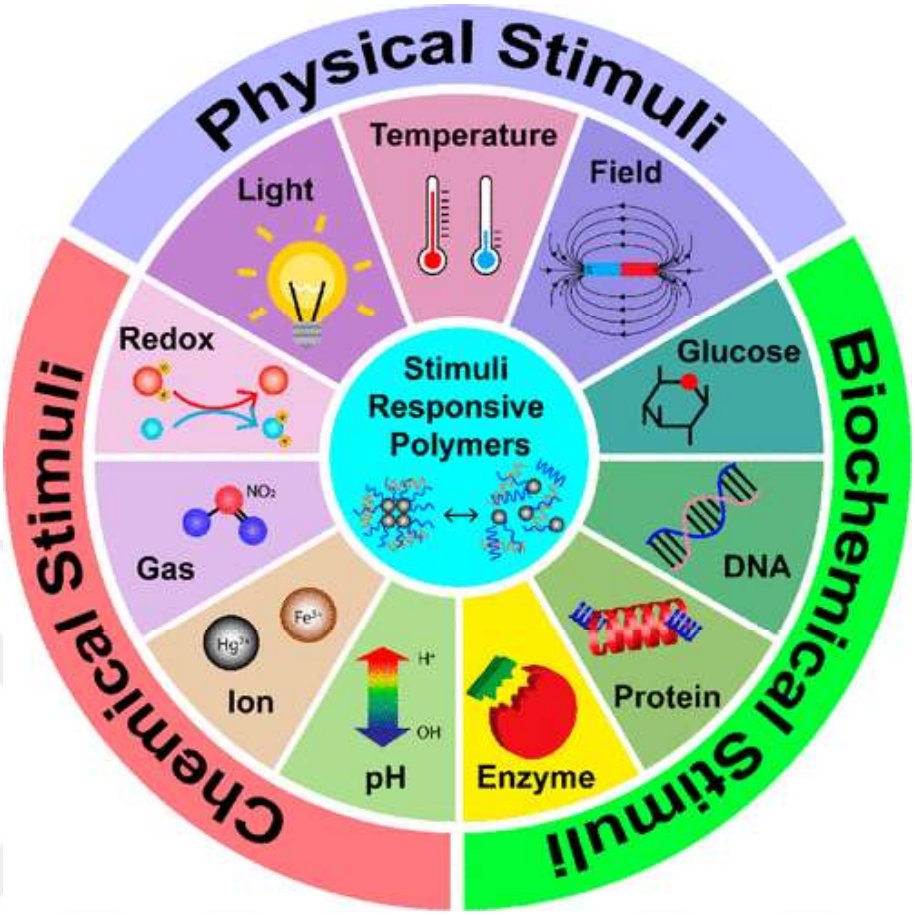

Figure 1.5. An overview of biochemical, physical, and chemical stimuli used for stimuli-responsive polymers [24].

Stimuli-responsive hydrogels, also known as "smart" hydrogels, possess the remarkable ability to undergo significant and reversible changes in their physical properties in response to external stimuli such as temperature, pH, light, and electric fields (Figure 1.6) [24]. These transformations are primarily driven by changes in the polymer network structure and interactions within the hydrogel matrix. The chemistry behind these responsive behaviors is complex, involving various molecular mechanisms and crosslinking strategies.

One of the fundamental aspects of stimuli-responsive hydrogels is their ability to undergo phase transitions in response to specific triggers. For instance, temperature-responsive hydrogels can exhibit a lower critical solution temperature (LCST) or an upper critical solution temperature (UCST), at which they transition from a swollen, hydrated state to a collapsed, dehydrated state [25]. This behavior is often governed by the hydrophilic-hydrophobic balance of the polymer chains. Polymers such as poly(N-isopropylacrylamide)

(PNIPAM) are classic examples of materials that exhibit LCST behavior. The temperature-induced phase transition in PNIPAM hydrogels is a result of the disruption of hydrogen bonds between the polymer and water molecules, leading to a hydrophobic collapse of the polymer chains.

Redox-responsiveness, a crucial aspect of stimuli-responsive materials, plays a vital role in the development of advanced hydrogels for biomedical applications. Redox-responsive hydrogels are designed to undergo structural changes or degradation in response to specific redox conditions. These conditions often involve variations in the levels of reactive oxygen species (ROS) or other redox-active molecules within the body. This responsiveness is particularly advantageous in targeting diseased tissues, such as cancerous or inflamed areas, where redox conditions differ significantly from healthy tissues. By incorporating redox-sensitive linkages into the hydrogel network, these materials can achieve controlled degradation or drug release in response to the local redox environment, enhancing therapeutic efficacy and minimizing side effects.

In the context of hydrogel design, redox-responsive properties are typically introduced through the incorporation of disulfide bonds. Disulfide linkages can be cleaved under reductive conditions, allowing for controlled degradation or release of encapsulated therapeutic agents [26]. This mechanism is particularly useful in creating hydrogels that can release their payload in response to the high levels of glutathione present in the intracellular environment of cancer cells. By leveraging the redox gradient between the extracellular and intracellular environments, redox-responsive hydrogels can achieve targeted and efficient drug delivery. Additionally, the integration of redox-sensitive components into the hydrogel matrix can improve the material's mechanical properties and biocompatibility, making them suitable for various biomedical applications.

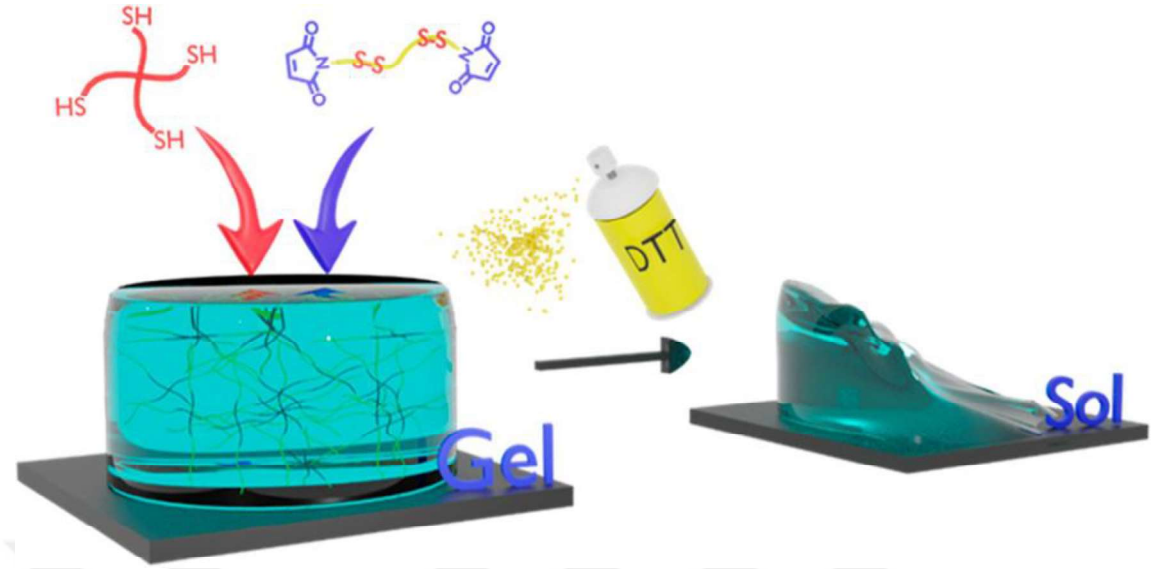

Figure 1.6. Schematic illustration of dissolvable HGs [26].

One notable example of redox-responsive hydrogels are the rapidly developing, dissolvable hydrogels shown in Figure 1.7 [26], which take use of the orthogonality of thiol–maleimide and thiol–disulfide exchange chemistry. This dual-crosslinking method offers a flexible platform for drug administration and tissue engineering applications by enabling the rapid generation of hydrogels that can dissolve under reductive circumstances. The creation of redox-responsive core-cross-linked micelles for the delivery of anticancer drugs is another noteworthy example, as shown in Figure 1.8 [27]. These micelles exhibit enhanced stability and redox-triggered drug release, ensuring that the therapeutic agents are released specifically at the target site, thereby improving the overall efficacy of the treatment. These advancements highlight the potential of redox-responsive hydrogels in revolutionizing drug delivery systems and tissue engineering strategies.

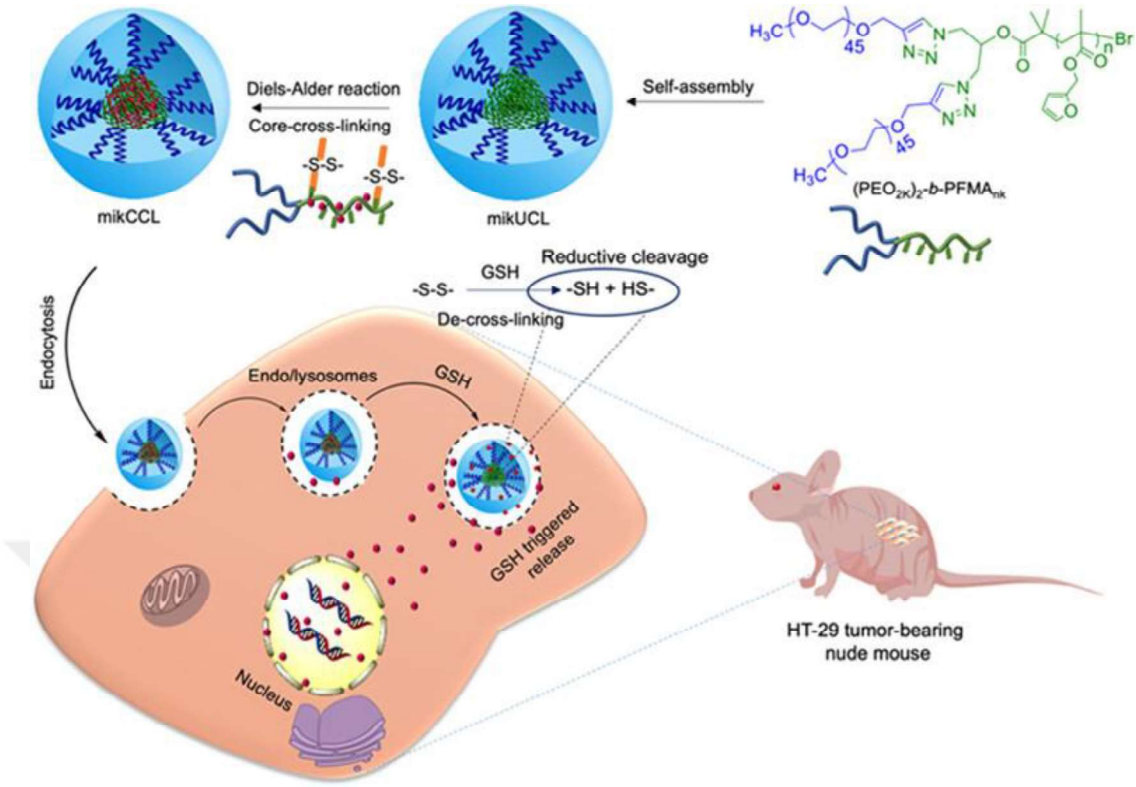

Figure 1.7. Schematic illustration of reduction-responsive intracellular drug delivery by the micelle structure [27].

pH-responsive hydrogels, on the other hand, rely on the ionization of acidic or basic functional groups within the polymer network. These hydrogels contain ionizable groups that can accept or donate protons in response to changes in pH, leading to alterations in the network's charge density and degree of swelling. For example, hydrogels composed of polymers with carboxylic acid groups, such as poly(acrylic acid) (PAA), can swell in basic conditions due to the ionization of carboxyl groups, which leads to electrostatic repulsion between the negatively charged polymer chains [28]. Conversely, in acidic conditions, the carboxyl groups are protonated, reducing the electrostatic repulsion and causing the hydrogel to collapse.

Light-responsive hydrogels leverage the ability of certain photochromic or photoreactive moieties to change their conformation or chemical state upon exposure to specific wavelengths of light. These photo-induced transformations can trigger changes in the hydrogel's swelling behavior, mechanical properties, or network structure. For instance, azobenzene-containing hydrogels can undergo reversible cis-trans isomerization upon

exposure to UV and visible light, respectively [29]. This isomerization can induce significant changes in the polymer network's conformation and, consequently, the hydrogel's physical properties.

Electric field-responsive hydrogels, also known as electro-responsive hydrogels, can undergo deformation or changes in their swelling behavior when subjected to an electric field. The mechanism behind this responsiveness is often attributed to the electrophoretic movement of charged species within the hydrogel or the electrostatic interactions between charged polymer chains [30]. Hydrogels containing polyelectrolytes, such as poly(2-acrylamido-2-methylpropane sulfonic acid) (PAMPS), can exhibit electro-responsive behavior due to the presence of mobile ions within the polymer network. When an electric field is applied, these ions migrate, leading to changes in osmotic pressure and, subsequently, the hydrogel's volume and mechanical properties.

The functionality of hydrogels is closely tied to their chemical composition and the design of their polymer networks. Crosslinking is a critical aspect of hydrogel chemistry that influences their mechanical strength, swelling behavior, and responsiveness [31]. Crosslinking can be achieved through various methods, including covalent bonding, physical entanglement, and ionic interactions. Covalent crosslinking involves the formation of stable chemical bonds between polymer chains, resulting in a permanent network structure. This method provides robust mechanical properties and structural integrity but can limit the hydrogel's ability to undergo large, reversible deformations.

Physical crosslinking, in contrast, relies on non-covalent interactions such as hydrogen bonding, hydrophobic interactions, and van der Waals forces to form a network. These interactions are typically weaker and reversible, allowing for dynamic changes in the hydrogel's structure in response to environmental stimuli. Hydrogels formed through physical crosslinking often exhibit greater flexibility and responsiveness compared to their covalently crosslinked counterparts.

Ionic crosslinking involves the use of multivalent ions to link polymer chains through electrostatic interactions. This method is commonly employed in the synthesis of alginate-based hydrogels [32], where divalent cations such as calcium ions are used to crosslink the

anionic alginate chains. Ionic crosslinking can provide a balance between mechanical strength and responsiveness, making it a versatile approach for designing stimuli-responsive hydrogels.

The incorporation of functional groups and responsive moieties into the polymer backbone or side chains is another key strategy for enhancing the functionality of hydrogels. Functional groups such as amines, carboxyls, and hydroxyls can participate in various chemical reactions, enabling the hydrogel to undergo specific transformations or interact with other molecules. Responsive moieties, such as azobenzenes, spiropyrans, and ferrocene, can impart hydrogel with the ability to respond to light, pH, or redox conditions, respectively.

The spatial distribution and density of these functional groups and responsive moieties within the hydrogel network play a crucial role in determining the material's overall behavior. For instance, a high density of ionizable groups can enhance the hydrogel's sensitivity to pH changes [33], while a uniform distribution of photo-responsive groups can ensure consistent light-induced transformations throughout the material [34]. The precise control over the placement and concentration of these functional entities is often achieved through advanced polymerization techniques, such as controlled/living radical polymerization, atom transfer radical polymerization (ATRP), and reversible addition-fragmentation chain transfer (RAFT) polymerization.

In addition to the inherent responsiveness of the polymer network, the design of composite hydrogels that incorporate nanoparticles, nanofibers, or other functional materials can further enhance their functionality. For example, the inclusion of magnetic nanoparticles can render the hydrogel responsive to magnetic fields, while the incorporation of conductive polymers can enable electro-responsive behavior [35]. These composite hydrogels benefit from the synergistic effects of the polymer matrix and the embedded functional materials, resulting in enhanced performance and versatility.

The applications of stimuli-responsive hydrogels span a wide range of fields, from drug delivery [36] and tissue engineering to soft robotics and sensors. In drug delivery, these hydrogels can provide controlled and targeted release of therapeutic agents in response to

specific physiological conditions, such as NIR-triggers changes in the temperature in inflamed tissues that can be seen in Figure 1.7 The ability to fine-tune the release profile by adjusting the hydrogel's chemistry and crosslinking density makes these materials highly adaptable for various therapeutic needs.

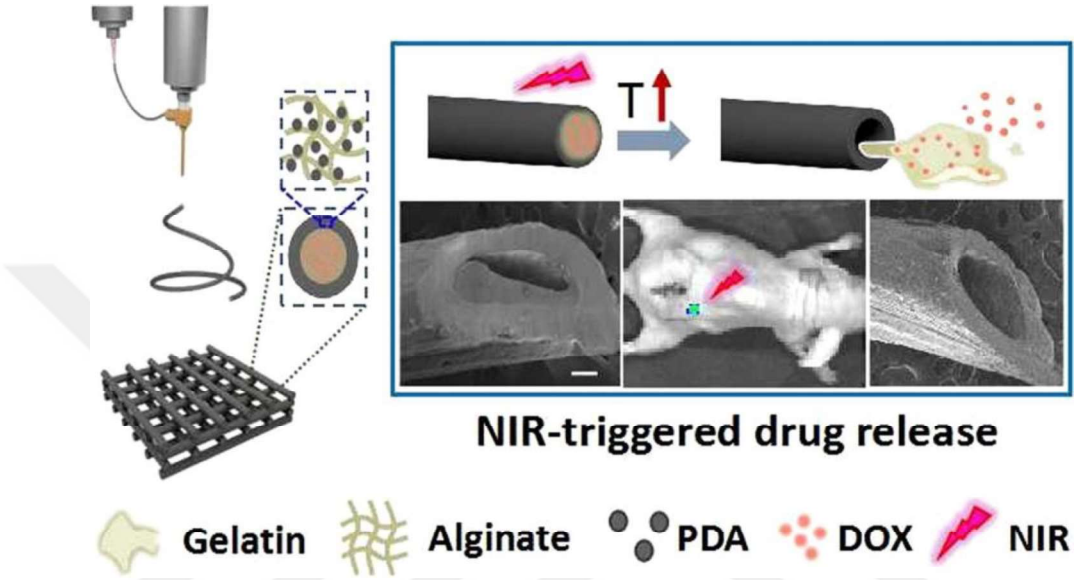

Figure 1.8. Schematic diagram of the co-axial 3D printing of core-shell fibers/scaffolds for localized cancer therapy. Drug released from the core hydrogels after NIR-induced reversible sol-gel transition [36].

In tissue engineering, stimuli-responsive hydrogels can serve as dynamic scaffolds that support cell growth and tissue regeneration while responding to the local microenvironment [37]. These hydrogels can mimic the natural extracellular matrix by providing biochemical and mechanical cues that guide cell behavior. For instance, hydrogels that respond to enzymatic activity can undergo controlled degradation, allowing for gradual tissue remodeling and integration with the host tissue. The development of sensors based on stimuli-responsive hydrogels is another area of significant interest. These sensors can detect changes in environmental conditions, such as temperature, pH, or the presence of specific chemicals, by undergoing measurable changes in their physical properties [38]. For example, hydrogels that swell or shrink in response to specific analytes can be used to create highly sensitive and selective sensors for biomedical diagnostics, environmental monitoring, and industrial applications.

2. AIM OF THE STUDY

The objective of this study is to design, synthesize, characterize, and evaluate novel biodegradable and functionalizable hydrogels that are 3D-printed and stimuli-responsive. The primary focus is to create a hydrogel system that seamlessly integrates biodegradability, functionalizability, and responsiveness to specific stimuli, suitable for advanced biomedical applications such as drug delivery and tissue engineering. This research aims to address the multifaceted challenges in developing a hydrogel that combines these critical properties effectively. In this study, the biodegradability aspect of the hydrogel system is derived from polyethylene glycol (PEG) polymers, which are well-known for their biocompatibility and degradable nature. PEG provides a foundation that is inherently non-toxic and can be broken down within the body, making it an ideal candidate for creating biodegradable hydrogels. The challenge lies in ensuring that the hydrogel maintains structural integrity while being biodegradable. This study will focus on optimizing the balance between degradation rate and mechanical stability to ensure that the hydrogels can support tissue regeneration processes without premature breakdown or excessive rigidity.

The stimuli-responsive nature of the hydrogels is engineered through the incorporation of redox-responsive disulfide linkages. Disulfide bonds are known for their ability to undergo reversible cleavage in response to redox conditions, a property that is harnessed to create hydrogels that can respond to specific physiological environments. The redox responsiveness is particularly significant for applications in drug delivery, where controlled release of therapeutic agents can be achieved in response to the local redox environment, such as those present in inflamed or cancerous tissues. The study aims to meticulously design the redox-responsive segments to ensure a precise and predictable response to the targeted stimuli, thereby enhancing the efficacy and safety of the hydrogel for biomedical applications. Functionalizability is another critical aspect of this hydrogel system, primarily facilitated by the disulfide linkages. The ability to functionalize hydrogel allows for the incorporation of various bioactive molecules, which can enhance the material's interaction with biological systems. In this work, the study will explore the potential for functionalization through the introduction of bioactive peptides, proteins, or other signaling molecules that can be conjugated via the disulfide bonds. The objective is to create a versatile

platform that can be tailored to specific applications by modifying the surface chemistry of the hydrogel, thereby enhancing cell adhesion, proliferation, and differentiation for tissue engineering applications.

The PEG-disulfide crosslinker, synthesized in-house and referred to as PEGSSDMa, is a central component of this hydrogel system. In this study, the custom synthesis of this crosslinker allows for precise control over the molecular architecture of the hydrogel, ensuring that the disulfide linkages are optimally positioned to impart both redox responsiveness and functionalizability. The study aims to characterize the PEGSSDMa crosslinker in detail, evaluating its effectiveness in forming stable hydrogels and its responsiveness to redox conditions. The synthesis process will be optimized to ensure reproducibility and scalability, essential for potential clinical applications.

Extruder-based 3D printing technology is employed to fabricate the hydrogel constructs. The choice of extrusion-based printing is driven by its ability to produce highly precise and complex structures, essential for creating scaffolds with defined geometries and internal architectures. In this research, the study aims to optimize the printing parameters, such as nozzle diameter, printing speed, and extrusion pressure, to achieve consistent and high-resolution hydrogel constructs. The mechanical properties and structural integrity of the printed hydrogels will be thoroughly evaluated to ensure they meet the requirements for their intended applications.

Gellan gum is introduced to the hydrogel formulation to increase the viscosity of the precursor solution. In this study, viscosity is a critical parameter in 3D bioprinting, as it affects the printability and structural fidelity of the printed constructs. A higher viscosity ensures that the hydrogel maintains its shape during and after the printing process, reducing the likelihood of deformation or collapse. The study will explore the optimal concentration of gellan gum to achieve a balance between printability and mechanical properties, ensuring that the hydrogel can be printed with high precision while maintaining its structural integrity.

To further expand on the use of PEGSSDMa, this study will delve into the specific attributes that make it a critical component of the hydrogel network. The PEGSSDMa crosslinker is designed to introduce disulfide bonds within the hydrogel structure, which

play a pivotal role in imparting redox-responsive characteristics. This study will investigate the stability of these disulfide bonds under various physiological conditions, ensuring that the hydrogels exhibit predictable and controlled degradation profiles. By fine-tuning the concentration and distribution of PEGSSDMa within the hydrogel matrix, this research aims to achieve a robust yet responsive material that can be precisely tailored for specific biomedical applications.

Moreover, the incorporation of PEGMEMa and PEGDMa in the hydrogel formulation brings additional benefits that will be thoroughly examined in this study. PEGMEMa, a methacrylated derivative of PEG, is employed to enhance the porosity of the hydrogels. Increased porosity is crucial for improving the swelling ratio and facilitating the encapsulation of cells or therapeutic agents. This study will systematically vary the concentration of PEGMEMa to optimize the pore size distribution within the hydrogel matrix, aiming to achieve the optimal balance between mechanical integrity and permeability.

On the other hand, PEGDMa, another methacrylated PEG derivative, is introduced to provide additional crosslinking within the hydrogel network. The dual-crosslinking strategy, combining PEGSSDMa and PEGDMa, is expected to enhance the mechanical stability of the hydrogels, making them more resilient under physiological conditions. This study will investigate the synergistic effects of PEGDMa and PEGSSDMa on the overall properties of the hydrogels, aiming to develop a material that is both strong and responsive.

In conclusion, this study aims to develop a versatile and advanced hydrogel system that combines biodegradability, functionalizability, and stimuli-responsiveness, tailored for 3D printing applications. By leveraging the unique properties of PEG, disulfide linkages, and advanced printing technologies, this research seeks to create a new class of hydrogels with significant potential for clinical applications in drug delivery and tissue engineering. Through systematic synthesis, characterization, and evaluation, this study aims to address the critical challenges in hydrogel design and pave the way for innovative biomedical solutions.

3. EXPERIMENTAL

3.1. Materials

Diethyl ether were purchased from Merck. 1,4-Dithio-dl-threitol (DTT) (98%) were purchased from Alfa Aesar. Gellan Gum (G434) was purchased from PhytoTech Labs. 4-(Dimethylamino)pyridine (DMAP, >99%), 3,3′-dithiodipropanoic acid (95%), N,N′-dicyclohexylcarbodiimide (DCC), lithium phenyl-2,4,6-trimethylbenzoylphosphinate (LAP, 95%), PEG (4 kDa), poly(ethylene glycol) diacrylate (PEGDA, Mn=550), poly(ethylene glycol) methyl ether methacrylate (PEGMEMA, Mn=950), toluene were purchased from Sigma-Aldrich. 2-[3-[(2-Carboxyethyl)dithio]-1-oxopropoxy]ethyl 2-methyl-2-propenoate (HEMA-SS) [39] was obtained using literature procedures.

3.2. Methods

Ultra-pure water was obtained via MilliQ Water Purification System (Merck Millipore, USA). NMR analysis was carried out using a 400 MHz Bruker spectrometer. The surface morphology of hydrogels was examined using scanning electron microscopy (SEM) (JEOL NeoScope JCM-500, with an accelerating voltage of 10 kV). FTIR spectroscopy measurements were performed with a Thermo Scientific Nicolet 380 FTIR spectrometer. The mechanical properties of hydrogels were analyzed using a rheometer (Anton PAAR MCR 302). UV-vis spectrophotometer measurements were carried out using Thermo Scientific Nanodrop 2000 spectrophotometer and a Varian Cary Eclipse, Agilent, USA).

3.3. Synthesis of Hydroxyethyl Methacrylate Disulfide (HEMA-SS) Acid

3,3′-Dithiodipropanoic acid (2.00 g, 0.010 mol), HEMA (0.50 g, 0.004 mol), and DMAP (0.352 g, 0.003 mol) were added to a round-bottom flask and dissolved in anhydrous dichloromethane (35 mL). DCC (1.98 g, 0.010 mol) was dissolved in dichloromethane (25 mL) in another flask. The solution of the second flask was slowly added to the mixture in the first flask that waited in ice. The combined reaction mixture was stirred at room temperature for 24 h. Dichloromethane (30 mL) was added to the reaction mixture, and then

the precipitated dicyclohexylurea (DCU) was removed by filtration. Purification using column chromatography on SiO2 using CH2Cl2 and EtOAc (1:1) as eluents yielded the pure product (2.12 g, 68%). 1H NMR (CDCl3, δ, ppm), 6.13 (s, 1H, C═CH2), 5.60 (s, 1H, C═CH2), 4.36 (t, 4H, OCH2CH2O), 2.92 (t, 4H, SCH2CH2), 2.77 (t, 4H, COCH2CH2), 1.95 (s, 3H, CH3C═CH2).

3.4. Synthesis of HEMA-SS-Terminated PEG Polymer

HEMA-SS acid (0.33 g, 1.025 mmol), PEG (4 kDa, 1.02 g, 0.256 mmol), and DMAP (0.06 g, 0.513 mmol) were added to a round-bottom flask and dissolved in dichloromethane (2 mL). DCC (0.21 g, 1.025 mmol) was added to another round-bottom flask and dissolved in dichloromethane (1 mL). The first solution was waited in ice, and the second solution was added to the ice-cold mixture drop by drop, and the reaction was stirred at room temperature for 24 h. Dichloromethane (5 mL) was added to the reaction mixture, the precipitated dicyclohexylurea (DCU) was removed by filtration. The amount of solvent was reduced by evaporation and the concentrated solution was precipitated in isopropyl alcohol. Precipitated pure product yielded (0.94 g, 79%). 1H NMR (CDCl3, δ, ppm), 6.13 (s, 2H, C═CH2), 5.60 (s, 2H, C═CH2), 4.35 (t, 4H, OCH2CH2), 4.25 (t, 4H, CH2CH2O), 3.36–3.81 (broad s, 360 H), 2.92 (t, 8H, SCH2CH2), 2.76 (t, 8H, COCH2CH2), 1.94 (s, 3H, CH3C═CH2).

3.5. Preparation and Characterization of the HGs

HGs were prepared by combining the two polymer solutions. Shortly, HEMA disulfide-terminated telechelic PEG polymer (50 mg), PEGDA (50/100/6 mg), PEGMEMa (50 mg) and GG (15 mg) were dissolved in 800 µL of deionized water. Solutions were mixed for 2 h. In another pot, LAP initiator dissolved in 200 µL of deionized water and then added to the polymer solution. The final mixture was put under UV light (365 nm) to form hydrogels. To ensure high interchain coupling, the mixture was waited under UV light for 1 h. Lyophilized HG disks (ca. 115 mg) were dipped in deionized water at 37 °C. The HG samples were periodically weighed after removing excess water from their surface using tissue paper. The water absorption was recorded until no increase in mass was noticeable. Swelling ratio percentages were calculated using (Ms – Mdry)/Mdry × 100, where Mdry and Ms refer to the weight of dry and swollen HGs, respectively. The linear viscoelastic limit

regime (LVR) and degradation profiles of HGs were recorded using an Anton Paar MCR 302 rheometer. A 15 mm diameter plate was utilized for the tests. The strain sweep test was performed to determine the LVR of HGs. Nonlinear strain regions pointed out a breakdown in HGs. It can be verified the lower frequency limit at which gel-like behavior is observable with the frequency sweep test. The determination of the frequency range for time sweep was made by frequency sweep tests with an appropriate angular frequency range (0.1-100 rad/s). The determination of the strain was made by the amplitude sweep tests with an appropriate strain value range (0.01-100 %). To track the degradation process, a time sweep test with a 1% strain and an angular frequency of 10 rad/s was used. A swollen HG was placed between heated rheometer plates and compress to 2 mm. Then gel surrounded by either glutathione solution or DTT in a time sweep test. For the purpose of the degradation experiments, a closed chamber was used to reduce any potential impact of solvent loss from vaporization.

3.6. Degradation of the HGs

Pieces of the disk-shaped HGs were kept at 37 °C in a thermal shaker (200 rpm) in 1 mL of PBS solution and 10 mM DTT containing 1 mL of PBS solution. After gelation, HG disks (1 cm diameter, 5 mm thick) were placed in an Eppendorf tube with 1 mL of deionized water and DTT (10 mM DTT in deionized water). The degradation process of bulk HGs for 24 h was recorded using a digital camera.

4. RESULTS AND DISCUSSION

4.1. Synthesis and Characterization of Disulfide Methacrylate-Terminated PEG Polymer

The telechelic PEG-based polymeric component containing methacryalte functional groups linked through a disulfide linker was derived from a readily available HEMA binded disulfide containing acid, as seen in Figure 4.1. To yield the desired chain-end functionality, the HEMA was linked to 3,3′-dithiodipropanoic acid through esterification. The composition and purity of the synthesized molecule were confirmed using ^{1}H NMR spectroscopy in Figure 4.2a and ^{13}C NMR spectroscopy in Figure 4.2b. The ^{13}C NMR spectrum exhibited the presence resonances at 176.8, 171.5 and 167.2 ppm belonging to carbonyl carbons confirming the three different carbonyl carbons which is in HEMA-SS acid structure. The esterification reaction was used for coupling this fragment with a linear PEG polymer to make disulfide-methacrylate ended telechelic PEG polymer as an HG precursor, as seen in Figure 4.1. The composition and purity of the PEG-SS-DMa in were confirmed using ^{1}H NMR spectroscopy in Figure 4.3a and ^{13}C NMR spectroscopy in Figure 4.3b. In the ^{13}C NMR spectrum of PEGSSDMa, the resonances at 69.0 and 63.9 ppm belonging to PEG carbons that adjust to ester and at 171.6 ppm belonging to carbonyl that binded to PEG polymer were evident. Additionally, Figure 4.4a's FTIR spectrum displays a broad peak at 3420 cm^{-1}, originating from the PEG molecule's OH groups; nevertheless, Figure 4.4b's peak vanishing at the same wavenumbers indicates that the conversion was effective. In addition to this data, Figure 4.4b shows the creation of a new peak at around 1720 cm^{-1}, which represents the stretching vibration of the newly formed carbonyl.

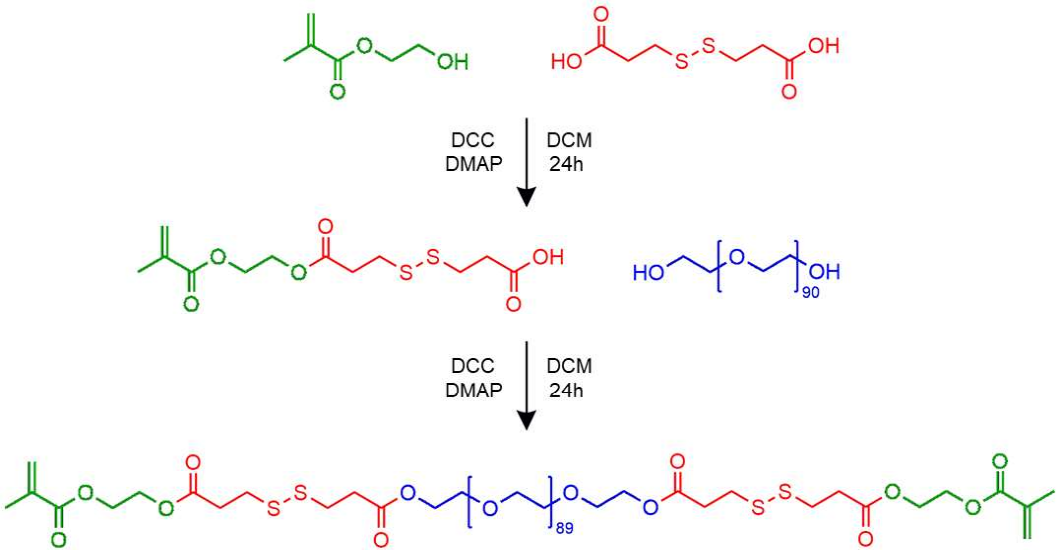

Figure 4.1. Synthesis of disulfide-containing PEGDMa crosslinker.

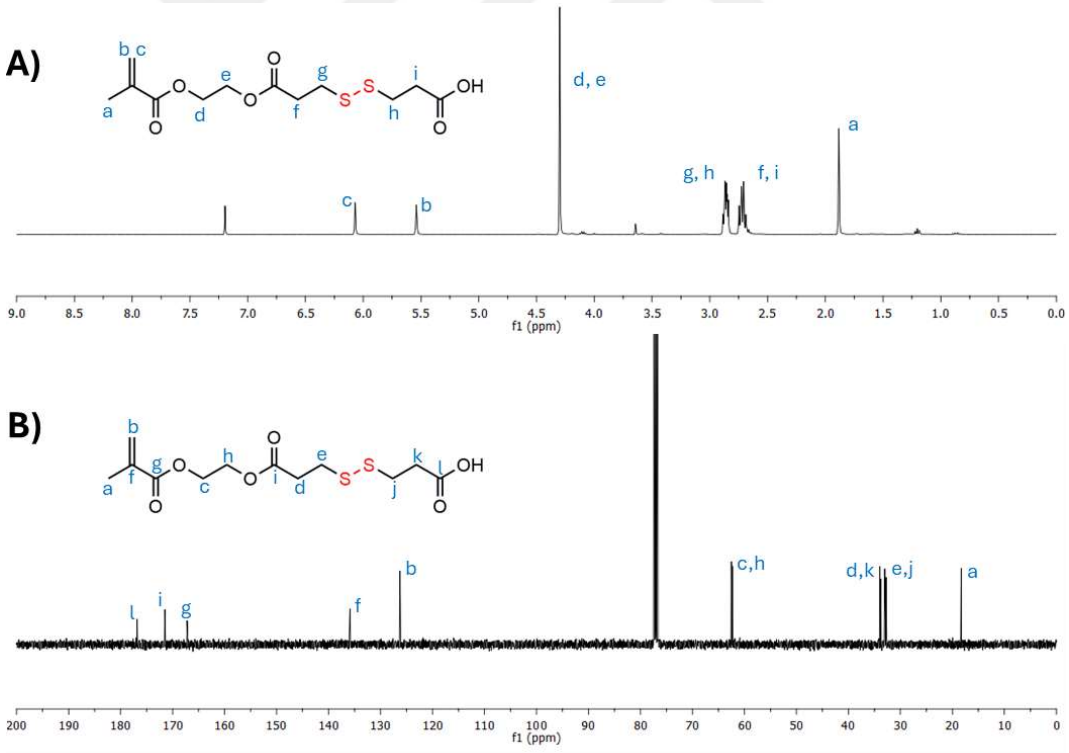

Figure 4.2. (a) ^{1}H NMR and (b) ^{13}C NMR spectra of the HEMA-disulfide acid.

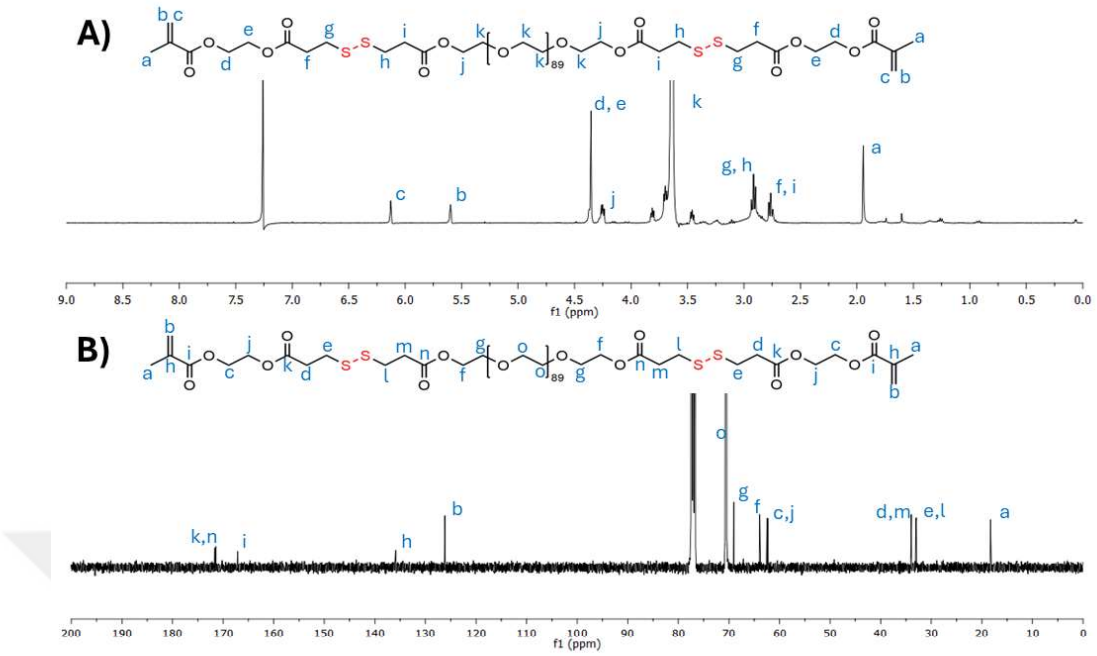

Figure 4.3. (a) ^{1}H NMR and (b) ^{13}C NMR spectra of the HEMA-SS-terminated PEG polymer.

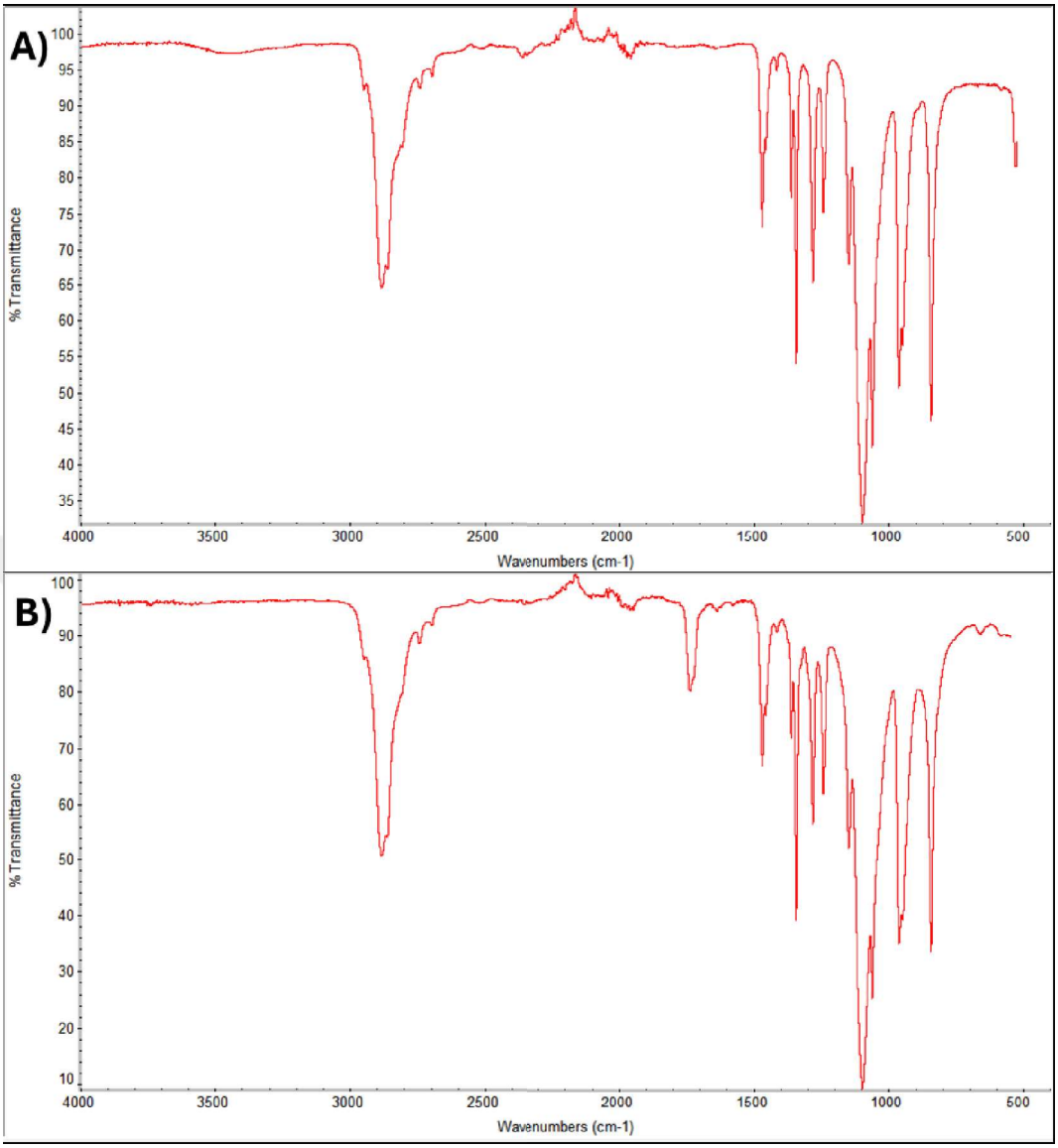

Figure 4.4. FTIR spectrum of (a) 4K PEG and (b) PEGSSDMa.

4.2. Preparation and Characterization of HGs

For the preparation of hydrogels, the disulfide-containing bis-methacryalate PEG polymer was mixed with PEG methyl ether methacrylate, PEG dimethacrylate polymer and gellan gum in water solution at room temperature, with the lithium phenyl-2,4,6-trimethylbenzoylphosphinate (LAP) as an UV initiator. Other characteristics are observed with varying monomer ratios that are shown Table 4.1. This table prepared in order to enhance the properties of the hydrogels, additional components such as PEGMEMa and

PEGDMa are incorporated. In this study, PEGMEMa is used to increase the pore size of the hydrogels, which is crucial for enhancing swelling ratios and facilitating cell encapsulation. The study aims to systematically investigate the effect of PEGMEMa concentration on the hydrogel's porosity and swelling behavior, optimizing the formulation to achieve the desired properties. On the other hand, PEGDMa is utilized as an additional crosslinker to stabilize the hydrogel network further. The dual-crosslinking approach with PEGDMa aims to enhance the mechanical stability of the hydrogels without compromising their degradability or responsiveness.

The UV crosslinking process is a crucial step in the fabrication of hydrogels, as it provides additional stability to the printed constructs. In this study, the parameters of the UV crosslinking process, such as exposure time (1h) and intensity (365nm), will be systematically optimized to achieve uniform crosslinking throughout the hydrogel matrix. The effect of UV crosslinking on the mechanical properties and redox responsiveness of the hydrogels will be thoroughly evaluated, ensuring that the final constructs meet the desired specifications for their intended applications. Figure 4.5a shows semi-transparent hydrogels formed within an hour of UV treatment. The morphology of the obtained hydrogels was investigated using scanning electron microscopy (SEM), and porous structures were observed in Figure 4.6. SEM images show that the absence of PEGDMa results in a more porous structure. Increases in the PEGSSDMa ratio additionally outcome in a more porous structure, as observed in Figures 4.6a and 4.6b. As expected for gels prepared with hydrophilic PEG polymers, hydrogels exhibited a rapid high-water uptake within minutes, as seen in Figure 4.7. As anticipated, the porous structure shown in Figure 4.6 is covered by water absorption over time.

Table 4.1. Hydrogels with different PEG-SS-DMa and PEGDMa ratios.

Sample	w/v (%) of PEGSSDMa	w/v (%) of PEGDMa	w/v (%) of PEGMEMa	w/v (%) of GG
HG1	10	0	5	1,5
HG2	10	5	5	1,5
HG3	5	5	5	1,5

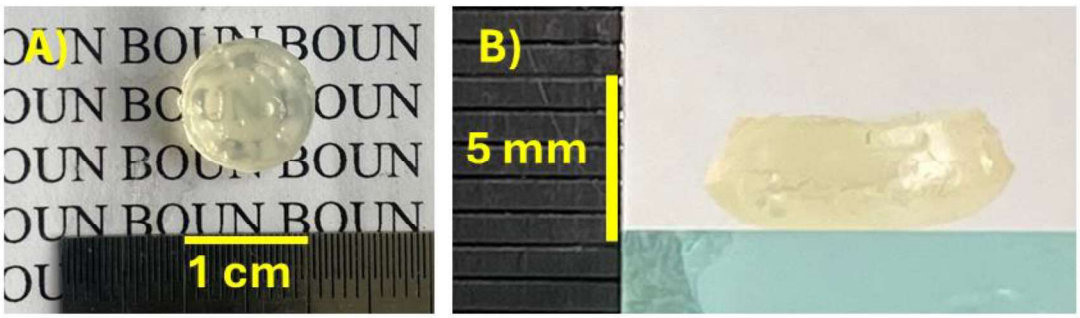

Figure 4.5. Photographic image of a wet HG1 hydrogel sample in front (a) and side (b).

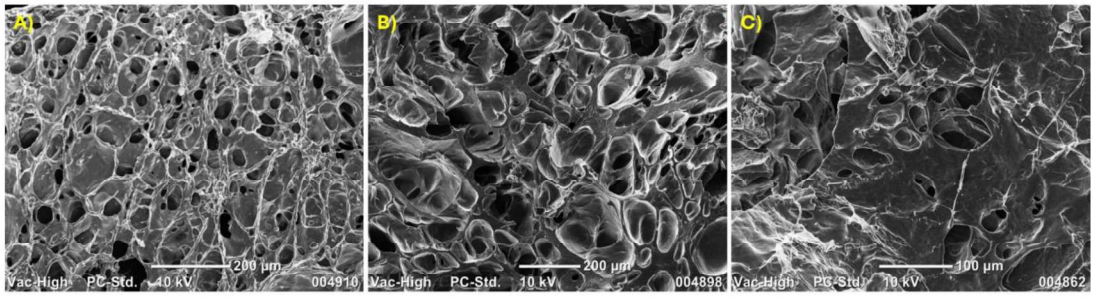

Figure 4.6. SEM pictures of hydrogels with different ratios (a) HG1, (b) HG2 and (c) HG3.

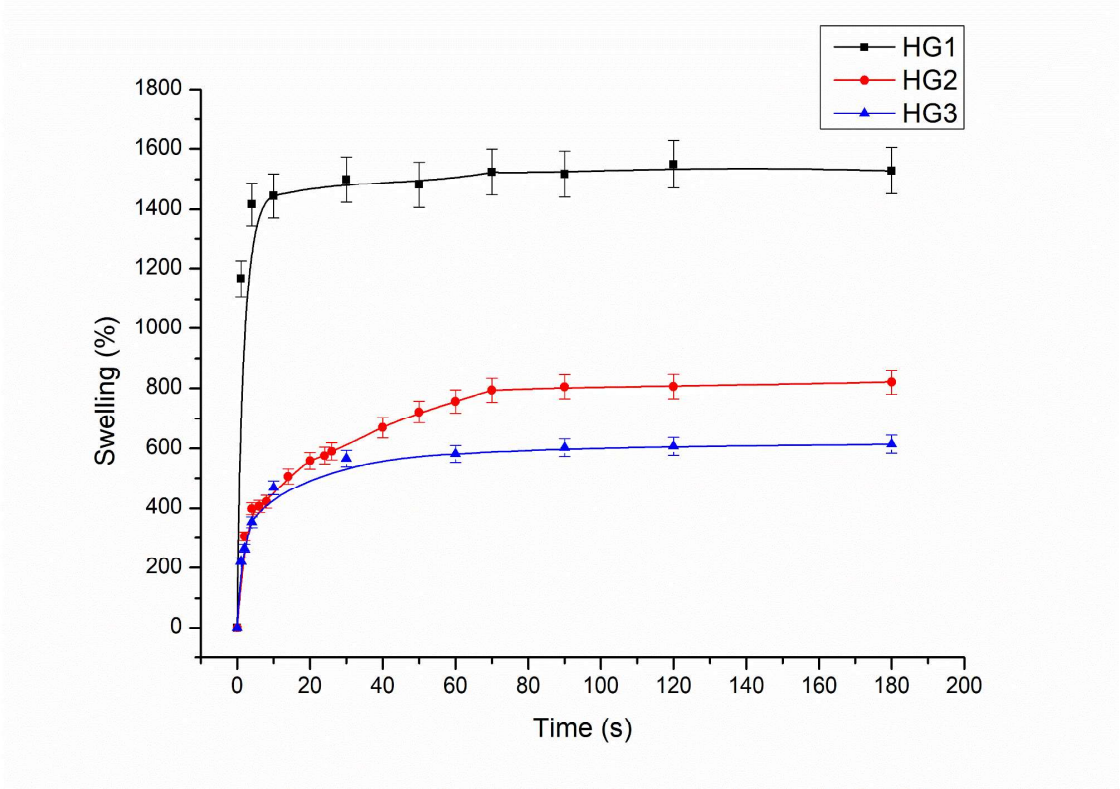

Figure 4.7. Swelling of HG1, HG2 and HG3 hydrogels.

4.3. Rheological Characterization of HGs

To investigate the printability profile of the HG solutions, rheological behaviors of a water-based HG solutions were studied via a strain sweep test and frequency sweep test. A strain sweep test was performed to investigate the linear viscoelastic limits of hydrogel solutions. When a 0.01 to 100% strain was applied to the hydrogel solution, a linear viscoelastic behavior was observed up to 4% strain under ten rad/s frequency in Figure 4.8a. Figure 4.8b demonstrates the response of hydrogel solutions to scaled frequency that was measured using a frequency sweep test from 0.01 to 25 rad/s by using a constant strain of 1%.

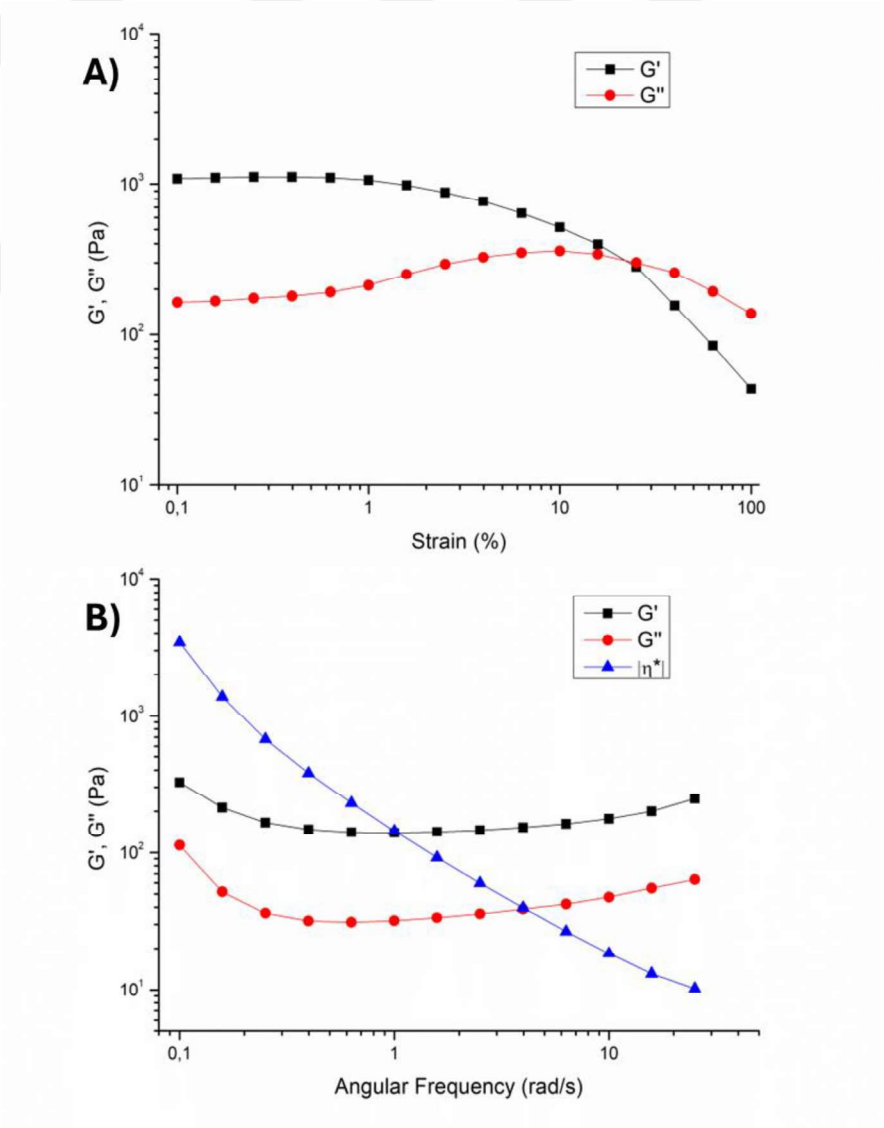

Figure 4.8. (a) Strain sweep and (b) frequency sweep test of HG1 hydrogel solution.

The rheological behaviors of a water-swollen HG were examined using a strain sweep test and a frequency sweep test in order to look into the stability profile of the HGs. To learn more about the linear viscoelastic limitations of hydrogels, a strain sweep test was performed. When a 0.01 to 100% strain was applied to the hydrogel, a linear viscoelastic behavior was observed up to 4% strain under ten rad/s frequency in Figure 4.9a, indicating a lack of structural breakdowns. Figure 4.9a shows the switch between storage and loss modulus prior to crosslinking with lower stresses. As predicted, the solution state has a higher complex viscosity, as seen in Figure 4.9b which is crucial for 3D-printing.

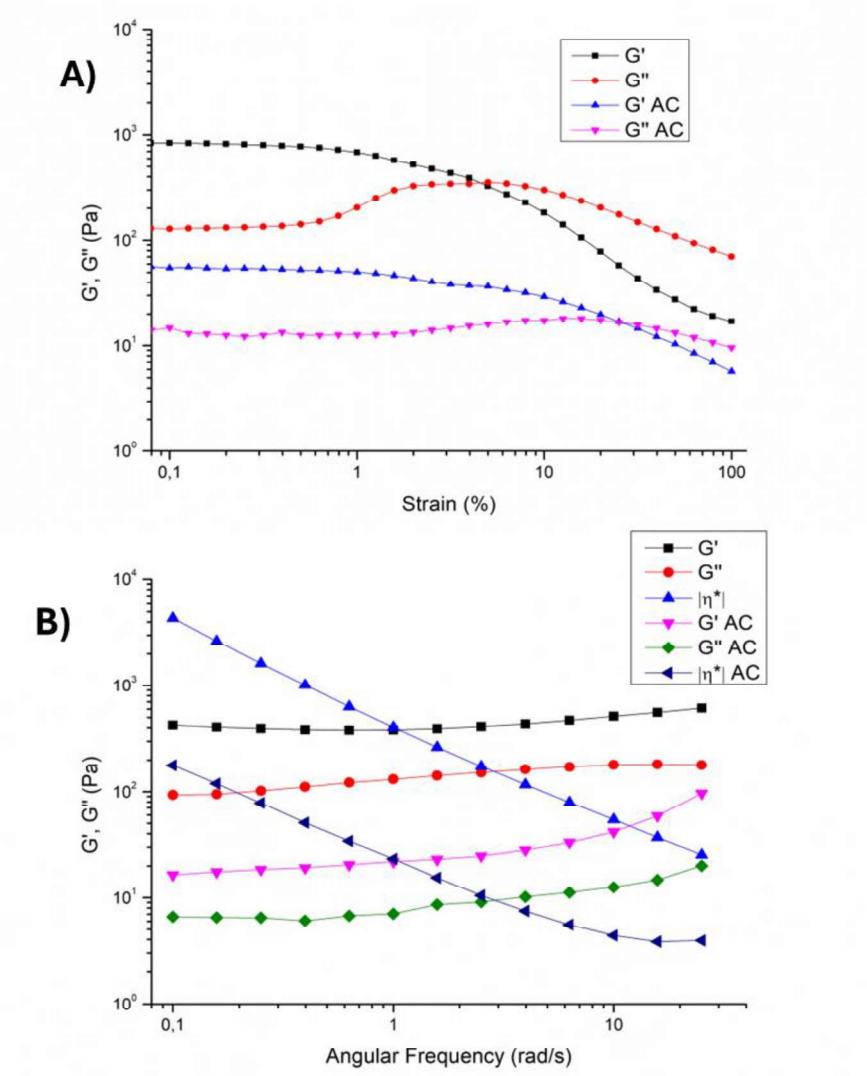

Figure 4.9. (a) Strain sweep and (b) frequency sweep test of HG1 hydrogel before and after crosslinking.

4.4. Degradation of HGs

To monitor the degradation behavior in reductive and nonreductive environments, HGs prepared with a fluorescent-o-methacrylate. To investigate the effect of dye loading on the rheological properties of HG, strain and frequency sweep tests were undertaken, and no significant change compared to the HGs was observed. Obtained fluorescent-o-methacrylate binded swollen disk-shaped hydrogel was cut into two pieces, and one of these pieces was immersed in purified water, while the other one was immersed in DTT solution (10 mM) at 37 $^{\circ}$C as seen in Figure 4.10. As expected, while the hydrogel kept in water did not show any visible degradation in the two-hour period, the hydrogel immersed in DTT solution degraded completely when absence of PEGDMa. Hence, as expected from the molecular design of these materials, they undergo rapid gelation to provide stable hydrogels and undergo rapid dissolution in the presence of a thiol-based reducing agent. Even so, Figure 4.11 shows that partial degradation of PEGDMa included hydrogels could be observed under the same circumstances over the course of 24 hours.

Degradation of hydrogels was also probed using the time sweep test in a rheometer. For the time sweep test, the hydrogel sample was placed between parallel plates, and the chamber around the hydrogel was filled with DTT or water solution. In Figure 4.12, it was observed that the elastic modulus of hydrogel remained constant when the chamber was filled with distilled water. However, a drastic decrease in elastic modulus was observed for the hydrogel that was incubated in the DTT solution.

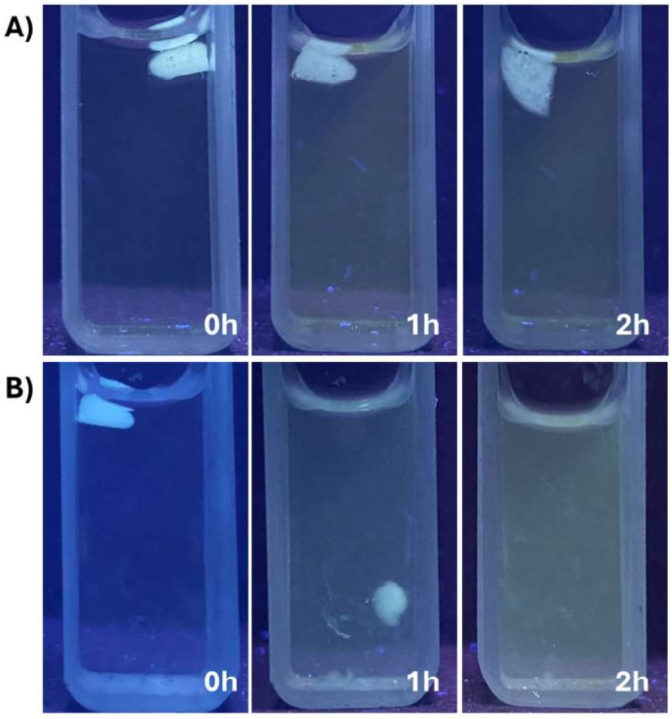

Figure 4.10. Photographic image of HG1 hydrogel sample in water (a) and in 10 mM DTT solution (b).

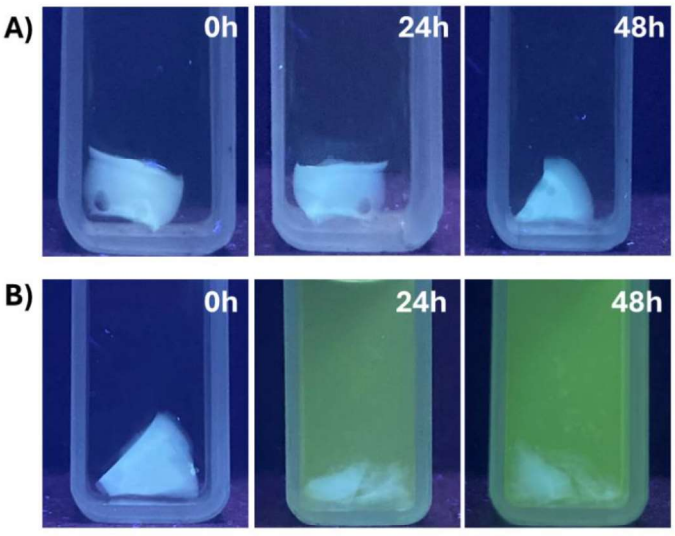

Figure 4.11. Photographic image of HG2 hydrogel sample in water (a) and in 10 mM DTT solution (b).

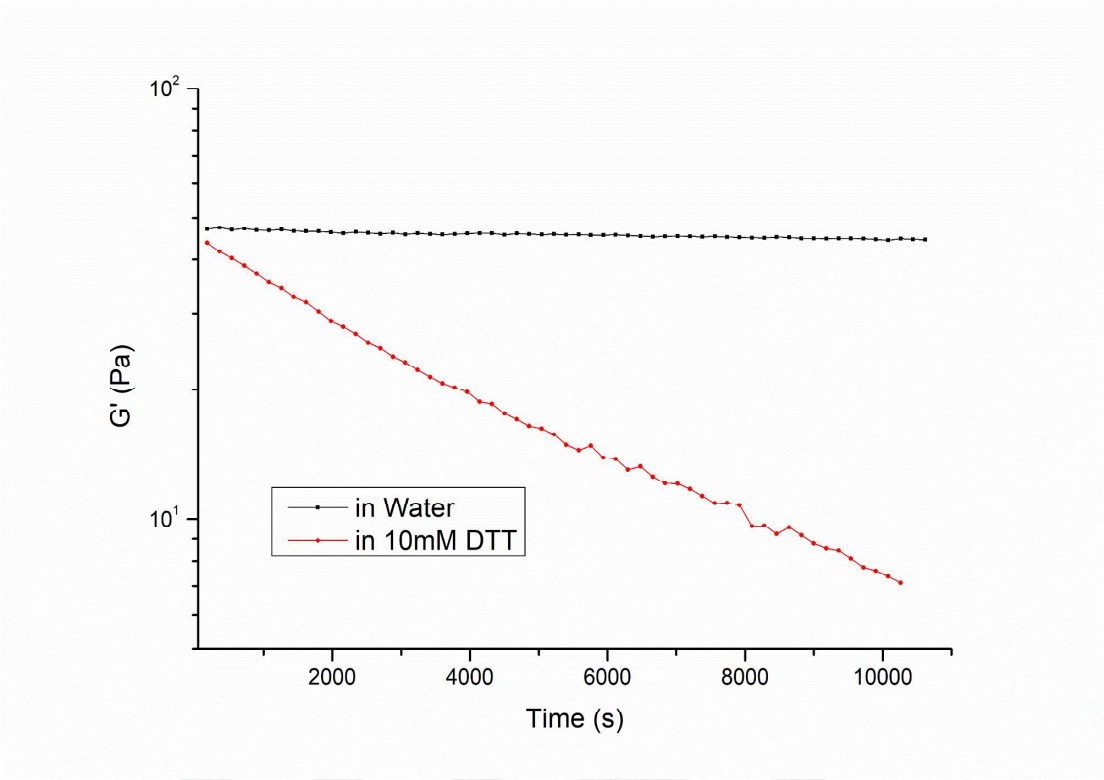

Figure 4.12. Time sweep test of HG1 hydrogel in the presence and absence of DTT.

4.5. Printability of HGs

Gellan gum, a polysaccharide derived from microbial fermentation, is added to the hydrogel formulation to modulate the viscosity of the precursor solution. In this study, the role of gellan gum in enhancing the viscosity will be explored in detail, as viscosity is a critical parameter in the 3D bioprinting process. High viscosity ensures that the hydrogel precursor maintains its shape during and after extrusion, preventing deformation and collapse of the printed constructs. This study will optimize the concentration of gellan gum to achieve the ideal balance between printability and mechanical properties, ensuring that the hydrogels can be printed with high precision while maintaining their structural integrity.

In conclusion, GG was added to the bioink solution as a thickening to help it keep its form. Various GG ratios (Table 4.2) as bioinks (BI) were tested in an attempt to find the optimal choice for 3D-bioprinting. A strain sweep test was performed to examine the rheological behaviors of a water-based HG solution in order to gain insights into the impact

of GG. To look into the linear viscoelastic properties of hydrogel solutions, a strain sweep test was conducted. Figure 4.13 shows that a linear viscoelastic behaviour was seen up to 10% and 60% strain under ten rad/s frequency when a 0.01 to 100% strain was applied to the hydrogel solution. Greater strain values suggest the possibility of obtaining a more stable form prior to crosslinking.

Table 4.2. Hydrogels with different gellan gum (GG) ratios.

Sample	w/v (%) of PEGDMa	w/v (%) of PEGMEMa	w/v (%) of GG
BInk1	5	5	1,5
BInk2	5	5	2

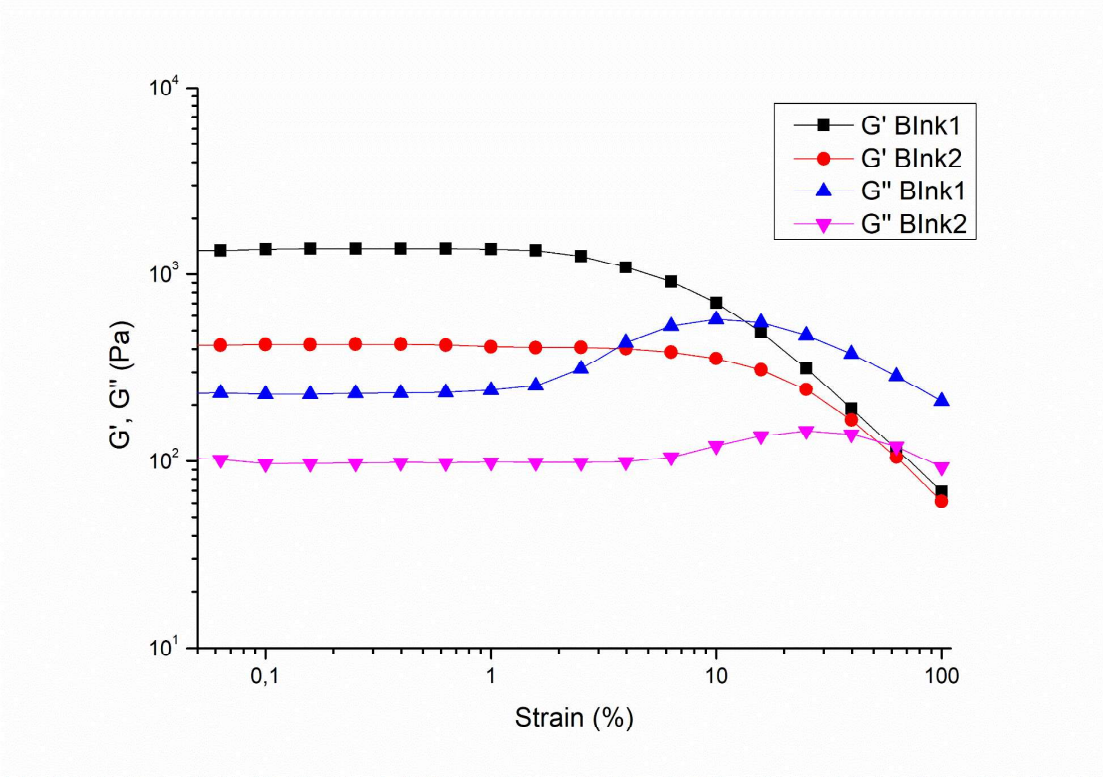

Figure 4.13. Strain sweep test of hydrogel solutions with different GG ratios (BInk1 and BInk2).

3D-printing performed with different shapes to try for further applications. As can be observed in Figure 4.14a and b, grid patterns are constructed. Also canal like concepts tried to mimic various tissues which can be seen in Figure 4.14c.

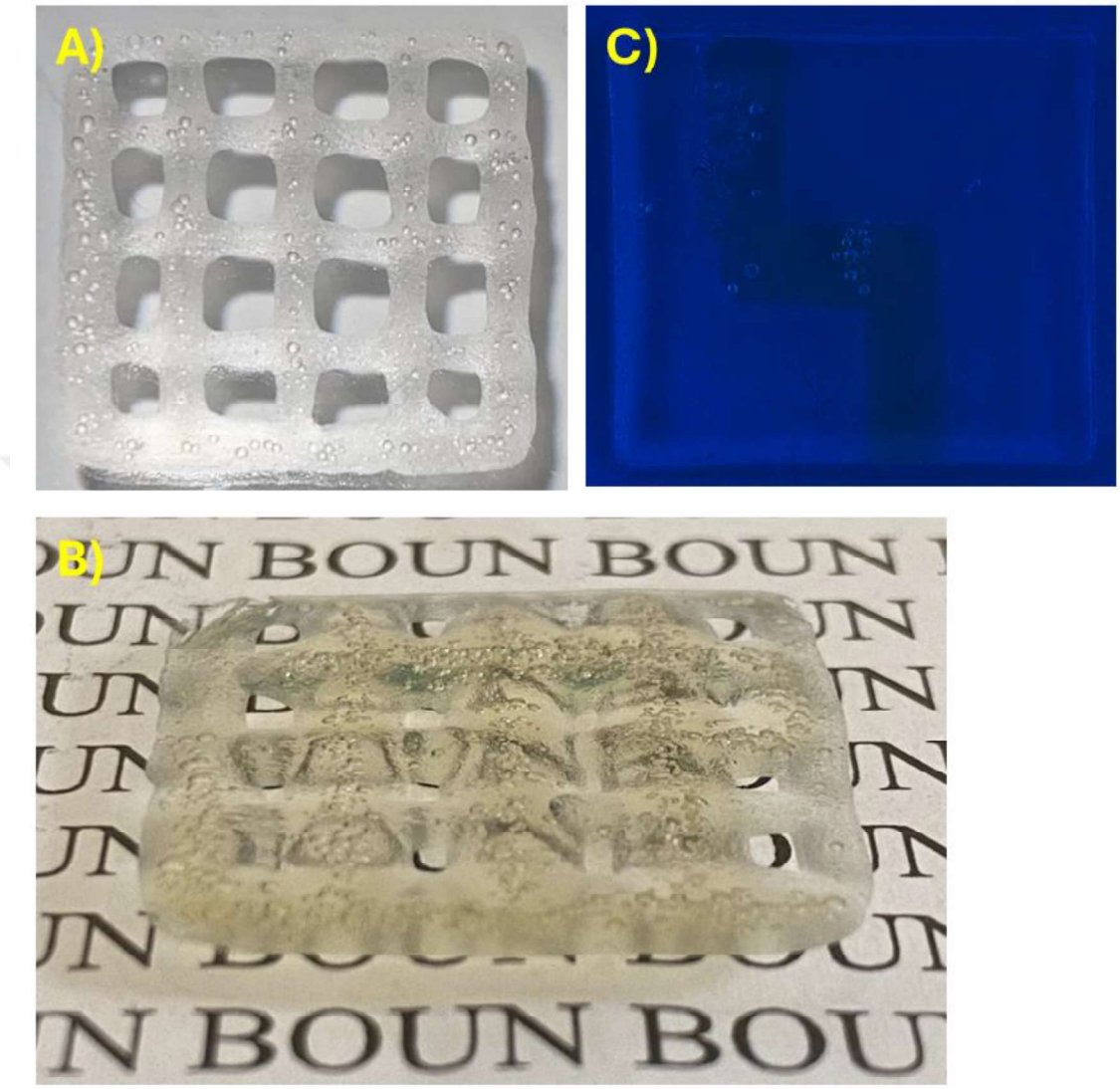

Figure 4.14. Photographic image of grit pattern up front (a), thick grit pattern on the side (b) made by HG1 and canal way (c) made outer filling with BInk1 and inner filling with HG1.

5. CONCLUSION

In this comprehensive study, we have successfully developed a new class of biodegradable, functionalizable, and stimuli-responsive hydrogels specifically designed for 3D printing applications, with potential applications in drug delivery and tissue engineering. The hydrogels were meticulously crafted using polyethylene glycol (PEG) polymers to ensure biodegradability, with redox-responsive disulfide linkages incorporated to provide stimuli-responsiveness. The custom-synthesized PEG-disulfide crosslinker (PEGSSDMa) was instrumental in imparting these unique properties, enabling precise control over the degradation and release profiles of the hydrogels.

The utilization of PEG polymers as the base material was crucial in achieving the desired biodegradability. PEG is well-known for its biocompatibility and ability to form hydrogels with tunable mechanical properties. By integrating disulfide linkages, we introduced redox-responsiveness into the hydrogel network. This functionality allows the hydrogels to respond to specific physiological stimuli, such as changes in the redox environment, which are commonly associated with pathological conditions like inflammation and cancer. The ability to fine-tune the degradation and release profiles through the PEGSSDMa crosslinker opens up new possibilities for creating highly targeted and efficient therapeutic systems.

The fabrication process leveraged extruder-based 3D printing technology, which offers high precision in producing complex structures with intricate designs. This method was chosen for its ability to create reproducible and customizable hydrogel constructs. Gellan gum was incorporated into the hydrogel precursor solution to enhance viscosity, a critical factor in maintaining the shape fidelity of printed constructs. The increased viscosity provided by gellan gum ensures that the hydrogel maintains its structural integrity during the printing process, preventing deformation and collapse. Post-printing, UV crosslinking was applied to further solidify the hydrogels, enhancing their mechanical stability and resistance to dissolution under physiological conditions.

The combination of PEGMEMa and PEGDMa was strategically employed to optimize the properties of the hydrogels. PEGMEMa was used to increase the porosity and swelling ratios of the hydrogels, which is particularly important for applications involving cell encapsulation and tissue engineering. Higher porosity facilitates better nutrient and oxygen diffusion, essential for cell viability and proliferation. PEGDMa was added as an additional crosslinker to further stabilize the hydrogel network, ensuring that the constructs remain intact over extended periods. This dual crosslinking approach provided a balance between mechanical strength and flexibility, making the hydrogels suitable for various biomedical applications.

The primary focus of this study was to evaluate the potential of these hydrogels for controlled drug release and tissue engineering. The redox-responsive nature of the hydrogels allows for the targeted release of therapeutic agents in response to specific physiological stimuli. For instance, in environments with altered redox states, such as those found in inflamed or cancerous tissues, the disulfide linkages within the hydrogel network can be selectively cleaved, triggering the release of encapsulated drugs. This targeted approach not only enhances the efficacy of the treatment but also minimizes the side effects associated with systemic drug administration.

In tissue engineering, the ability to functionalize the hydrogels with bioactive molecules offers a versatile platform for promoting cell adhesion, proliferation, and differentiation. The hydrogels can be tailored to create a microenvironment that closely mimics the natural extracellular matrix, providing the necessary cues for tissue regeneration. The combination of biodegradability and functionalizability makes these hydrogels ideal scaffolds for supporting the growth and development of new tissues. By incorporating growth factors, peptides, or other bioactive molecules, the hydrogels can be engineered to guide the behavior of encapsulated cells, enhancing their ability to form functional tissues.

The extruder-based 3D printing approach used in this study allowed for the precise fabrication of hydrogel constructs with complex geometries and intricate internal structures. This level of precision is essential for creating scaffolds that can support the growth of complex tissues, such as those found in the liver, heart, or bone. The ability to design and print customized hydrogel constructs opens up new possibilities for personalized medicine,

where scaffolds can be tailored to meet the specific needs of individual patients. Additionally, the 3D printing technology enables the rapid prototyping of different scaffold designs, facilitating the optimization of their properties for specific applications.

The incorporation of gellan gum into the hydrogel precursor solution was a key factor in achieving the desired printability. The increased viscosity provided by gellan gum ensures that the hydrogel maintains its shape during the printing process, preventing sagging or collapse. This is particularly important for creating scaffolds with complex geometries, where maintaining structural integrity is crucial. The use of UV crosslinking post-printing further enhanced the mechanical stability of the hydrogels, ensuring that they can withstand the forces encountered in physiological environments.

In this research, the synthesized hydrogels were characterized using a variety of techniques to assess their mechanical properties, degradation behavior, and stimuli-responsiveness. Rheological studies were conducted to evaluate the viscosity and flow behavior of the hydrogel precursor solutions, confirming their suitability for 3D printing. Mechanical testing was performed on the printed hydrogels to determine their tensile strength, elasticity, and compressive modulus, ensuring that they meet the requirements for their intended applications. Degradation studies were carried out to assess the rate at which the hydrogels break down under physiological conditions, providing insights into their potential longevity in vivo. Additionally, the stimuli-responsive behavior of the hydrogels was evaluated by exposing them to redox conditions and monitoring the release of encapsulated agents.

The findings from this study demonstrate the significant potential of these hydrogels for applications in drug delivery and tissue engineering. The ability to precisely control the degradation and release profiles, combined with the versatility of 3D printing, opens up new possibilities for creating advanced therapeutic systems. The redox-responsive nature of the hydrogels allows for the targeted release of drugs in specific physiological environments, enhancing the efficacy and safety of treatments. In tissue engineering, the ability to create customized scaffolds that support the growth and development of new tissues holds great promise for regenerative medicine.

In conclusion, this study represents a significant advancement in the development of multifunctional hydrogels for biomedical applications. By combining biodegradability, functionalizability, and stimuli-responsiveness, we have created a versatile hydrogel system that can be tailored for a wide range of applications. The use of extruder-based 3D printing technology allows for the precise fabrication of complex hydrogel constructs, paving the way for personalized medicine and advanced therapeutic solutions. Future research will focus on further optimizing the hydrogel formulations and exploring their in vivo applications, with the ultimate goal of translating these findings into clinical practice. This study provides a solid foundation for the development of innovative biomedical solutions that can address some of the most pressing challenges in healthcare today.

REFERENCES

1. Xiao, W., Gu, S., & Yuan, W., "Injectable Nanocomposite Hydrogels with the NIR-Triggered Low-Temperature Photothermal Effect and Low-Dose Antibiotic Release.", *ACS Applied Polymer Materials*, Vol. 5, No. 7, pp. 5200–5210, 2023.

2. Thambi, T., Jung, J. M., & Lee, D. S., "Recent Strategies to Develop pH-sensitive Injectable Hydrogels.", *Biomaterials Science*, Vol. 11, No. 6, pp. 1948–1961, 2023.

3. Sancar, T., Altinbasak, I., Sanyal, R., & Sanyal, A., "Electrospun Photothermally Active Graphene-Based Nanofibers with a Retro-Diels-Alder Reaction to Initiate Drug Release.", *European Polymer Journal/European Polymer Journal*, Vol. 210, pp. 112946, 2024.

4. Dreiss, C. A., "Hydrogel Design Strategies for Drug Delivery.", *Current Opinion in Colloid & Interface Science*, Vol. 48, pp. 1–17, 2020.

5. Altinbasak, I., Kocak, S., Sanyal, R., & Sanyal, A., "Redox-Responsive Nanogels for Drug-Delivery: Thiol–Maleimide and Thiol–Disulfide Exchange Chemistry as Orthogonal Tools for Fabrication and Degradation.", *Polymer Chemistry*, Vol. 14, No. 34, pp. 3897–3905, 2023.

6. F Hu, L., Zhang, Q., Li, X., & Serpe, M. J., "Stimuli-Responsive Polymers for Sensing and Actuation.", *Materials Horizons*, Vol. 6, No. 9, pp. 1774–1793, 2019.

7. Mano, J. F., "Stimuli-Responsive Polymeric Systems for Biomedical Applications.", *Advanced Engineering Materials*, Vol. 10, No. 6, pp. 515–527, 2008.

8. Horkay, F., & Basser, P. J., "Hydrogel Composite Mimics Biological Tissues.", *Soft Matter*, Vol. 18, No. 23, pp. 4414–4426, 2022.

9. Hong, Y., Zhou, F., Hua, Y., Zhang, X., Ni, C., Pan, D., Zhang, Y., Jiang, D., Yang, L., Lin, Q., Zou, Y., Yu, D., Arnot, D. E., Zou, X., Zhu, L., Zhang, S., & Ouyang, H., "A Strongly Adhesive Hemostatic Hydrogel for the Repair of Arterial and Heart Bleeds.", *Nature Communications*, Vol. 10, No. 2060, 2019.

10. Liu, Xiaowei, Haojie Yu, Li Wang, Zhikun Huang, Fazal Haq, Lisong Teng, Meijin Jin, Binbin Ding, X Liu, H Yu, L Wang, Z Huang, F Haq, L Teng, M Jin, and B Ding, "Recent Advances on Designs and Applications of Hydrogel Adhesives.", *Advanced Materials Interfaces*, Vol. 9, No. 2, pp. 2101038, 2022.

11. L Farazin, A., Shirazi, F. A., & Shafiei, M., "Natural Biomarocmolecule-Based Antimicrobial Hydrogel for Rapid Wound Healing: A Review.", *International Journal of Biological Macromolecules*, Vol. 244, pp. 125454, 2023.

12. Chimene, D., Lennox, K. K., Kaunas, R. R., & Gaharwar, A. K., "Advanced BioInks for 3D Printing: A Materials Science Perspective.", *Annals of Biomedical Engineering*, Vol. 44, No. 6, pp. 2090–2102, 2016.

13. Valls-Esteve, A., Tejo-Otero, A., Lustig-Gainza, P., Buj-Corral, I., Fenollosa-Artés, F., Rubio-Palau, J., De La Torre, I. B., Munuera, J., Fondevila, C., & Krauel, L., "Patient-Specific 3D Printed Soft Models for Liver Surgical Planning and Hands-On Training.", *Gels*, Vol. 9, No. 4, pp. 339, 2023.

14. Wu, D., Yu, Y., Tan, J., Huang, L., Luo, B., Lu, L., & Zhou, C., "3D Bioprinting of Gellan Gum and Poly (ethylene glycol) diacrylate Based Hydrogels to Produce Human-Scale Constructs with High-Fidelity.", *Materials & Design*, Vol. 160, pp. 486–495, 2018.

15. Raees, S., Ullah, F., Javed, F., Akil, H. M., Khan, M. J., Safdar, M., Din, I. U., Alotaibi, M. A., Alharthi, A. I., Bakht, M. A., Ahmad, A., & Nassar, A. A., "Classification, Processing, and Applications of Bioink and 3D Bioprinting: A Detailed Review.", *International Journal of Biological Macromolecules*, Vol. 232, pp. 123476, 2023.

16. Zhang, B., Korolj, A., Lai, B. F. L., & Radisic, M., “Advances in Organ-on-a-Chip Engineering.”, *Nature Reviews. Materials*, Vol. 3, No. 8, pp. 257–278, 2018.

17. Huang, G., Zhao, Y., Chen, D., Wei, L., Hu, Z., Li, J., Zhou, X., Yang, B., & Chen, Z., “Applications, Advancements, and Challenges of 3D Bioprinting in Organ Transplantation.”, *Biomaterials Science*, Vol. 12, No. 6, pp. 1425-1448, 2024.

18. Kong, Z., & Wang, X., “Bioprinting Technologies and BioINKs for Vascular Model Establishment.”, *International Journal of Molecular Sciences*, Vol. 24, No. 1, pp. 891, 2023.

19. Hosseinabadi, H. G., Nieto, D., Yousefinejad, A., Fattel, H., Ionov, L., & Miri, A. K., “Ink Material Selection and Optical Design Considerations in DLP 3D Printing.”, *Applied Materials Today*, Vol. 30, pp. 101721, 2023.

20. O’Shea, D. G., Hodgkinson, T., Curtin, C. M., & O’Brien, F. J., “An Injectable and 3D Printable Pro-Chondrogenic Hyaluronic Acid and Collagen Type II Composite Hydrogel for the Repair of Articular Cartilage Defects.”, *Biofabrication*, Vol. 16, No. 1, pp. 015007, 2023.

21. Ding, Q., Zhang, S., Liu, X., Zhao, Y., Yang, J., Chai, G., Wang, N., Ma, S., Liu, W., & Ding, C., “Hydrogel Tissue Bioengineered Scaffolds in Bone Repair: A Review.”, *Molecules/Molecules Online/Molecules Annual*, Vol. 28, No. 20, pp. 7039, 2023.

22. Li, W., Zhou, Z., Zhou, X., Khoo, B. L., Gunawan, R., Chin, Y. R., Zhang, L., Yi, C., Guan, X., & Yang, M., “3D Biomimetic Models to Reconstitute Tumor Microenvironment in Vitro: Spheroids, Organoids, and Tumor-on-a-Chip.”, *Advanced Healthcare Materials/Advanced Healthcare Materials*, Vol. 12, No. 18, 2023.

23. Shyam, R., Reddy, L. V. K., & Palaniappan, A., “Fabrication and Characterization Techniques of in Vitro 3D Tissue Models.”, *International Journal of Molecular Sciences*, Vol. 24, No. 3, pp. 1912, 2023.

24. Sun, X., Agate, S., Salem, K. S., Lucia, L., & Pal, L., “Hydrogel-Based Sensor Networks: Compositions, Properties, and Applications—A Review.”, *ACS Applied Bio Materials*, Vol. 4, No. 1, pp. 140–162, 2020.

25. Tanga, S., Aucamp, M., & Ramburrun, P., “Injectable Thermoresponsive Hydrogels for Cancer Therapy: Challenges and Prospects.”, *Gels*, Vol. 9, No. 5, pp. 418, 2023.

26. Altinbasak, I., Kocak, S., Sanyal, R., & Sanyal, A., “Fast-Forming Dissolvable Redox-Responsive Hydrogels: Exploiting the Orthogonality of Thiol–Maleimide and Thiol–Disulfide Exchange Chemistry.”, *Biomacromolecules*, Vol. 23, No. 9, pp. 3525–3534, 2022.

27. Kumar, P., Kim, S., Yadav, S., Jo, S., Yoo, S., Park, S., & Lim, K. T., “Redox-Responsive Core-Cross-Linked Micelles of Miktoarm Poly(ethylene oxide)-b-poly(furfuryl methacrylate) for Anticancer Drug Delivery.”, *ACS Applied Materials & Interfaces*, Vol. 15, No. 10, pp. 12719–12734, 2023.

28. Pourmadadi, M., Darvishan, S., Abdouss, M., Yazdian, F., Rahdar, A., & Díez-Pascual, A. M., “pH-Responsive Polyacrylic Acid (PAA)-carboxymethyl Cellulose (CMC) Hydrogel Incorporating Halloysite Nanotubes (HNT) for Controlled Curcumin Delivery.”, *Industrial Crops and Products*, Vol. 197, pp. 116654, 2023.

29. Pourbadiei, B., Adlsadabad, S. Y., Rahbariasr, N., & Pourjavadi, A., “Synthesis and Characterization of Dual Light/Temperature-Responsive Supramolecular Injectable Hydrogel Based on Host-Guest Interaction Between Azobenzene and Starch-Grafted β-cyclodextrin: Melanoma Therapy with Paclitaxel.”, *Carbohydrate Polymers*, Vol. 313, pp. 120667, 2023.

30. Hu, H., Li, D., Salim, T., Li, Y., Cheng, G., Lam, Y. M., & Ding, J., “Electrically Driven Hydrogel Actuators: Working Principle, Material Design and Applications.”, *Journal of Materials Chemistry. C*, Vol. 12, No. 5, pp. 1565–1582, 2024.

31. Hennink, W., & Van Nostrum, C., “Novel Crosslinking Methods to Design Hydrogels.”, *Advanced Drug Delivery Reviews*, Vol. 64, pp. 223–236, 2012.

32. Tan, J., Luo, Y., Guo, Y., Zhou, Y., Liao, X., Li, D., Lai, X., & Liu, Y., “Development of Alginate-Based Hydrogels: Crosslinking Strategies and Biomedical Applications.”, *International Journal of Biological Macromolecules*, Vol. 239, pp. 124275, 2023.

33. Hollingshead, S., & Liu, J. C., “pH-Sensitive Mechanical Properties of Elastin-Based Hydrogels.”, *Macromolecular Bioscience*, Vol. 20, No. 4, 2020.

34. Deng, Y., Long, G., Zhang, Y., Zhao, W., Zhou, G., Feringa, B. L., & Chen, J., “Photo-Responsive Functional Materials Based on Light-Driven Molecular Motors.”, *Light, Science & Applications/Light: Science & Applications*, Vol. 13, No. 1, 2024.

35. Carayon, I., Gaubert, A., Mousli, Y., & Philippe, B., “Electro-Responsive Hydrogels: Macromolecular and Supramolecular Approaches in the Biomedical Field.”, *Biomaterials Science*, Vol. 8, No. 20, pp. 5589–5600, 2020.

36. Wei, X., Liu, C., Wang, Z., & Luo, Y., “3D Printed Core-Shell Hydrogel Fiber Scaffolds with NIR-Triggered Drug Release for Localized Therapy of Breast Cancer.”, *International Journal of Pharmaceutics*, Vol. 580, pp. 119219, 2020.

37. Amirthalingam, S., Rajendran, A. K., Moon, Y. G., & Hwang, N. S., “Stimuli-Responsive Dynamic Hydrogels: Design, Properties and Tissue Engineering Applications.”, *Materials Horizons*, Vol. 10, No. 9, pp. 3325–3350, 2023.